NASA Contract Report 182183

A MILLIMETER-WAVE TUNNELADDER TWT

FINAL REPORT

D. Wilson

Varian Associates, Inc.
Palo Alto, California

October 1988

Prepared for
Lewis Research Center
Under Contract NAS3-23347

NASA
National Aeronautics and Space Administration
Lewis Research Center
Cleveland, Ohio 44135
AC 216 433-4000

PREFACE

The effort reported here was supported by NASA Lewis Research Laboratory on Contract NAS 3-23347. During the course of the program, many people made significant contributions to the development of TunneLadder tubes.

- Arthur Karp guided the circuit design and consulted on the performance estimates.

- Andy Jacquez managed the program in its early stages and provided support on several aspects of the tube design.

- Dan Andker developed the circuit brazing techniques and designed many of the major subassemblies.

- Larry Nolan refined the brazing and assembly techniques, redesigned the rf windows, constructed most of the assemblies, including all of those used on the engineering model, and assembled and processed that tube.

- Max Mizuhara provided a great deal of support on the mechanical redesign used on the engineering model.

- David West and Gene Barreras also made significant contributions.

TABLE OF CONTENTS

1.0 INTRODUCTION

1.1 GENERAL INFORMATION

This report describes the work done on a traveling-wave amplifier intended for use in narrow-band, millimeter-wave space communications systems. The circuit developed for this application is derived from a concept by Arthur Karp[1] and is, therefore, referred to as a Karp-type circuit. The Karp concept was further developed at NASA, Lewis Research center. The result is an axially uniform structure composed of two ladder-like, nonplanar arrays of conductors surrounding a beam hole, loaded by waveguide ridges and supported by dielectric blocks.

This type of structure can be relatively inexpensive, compared to coupled-cavity slow-wave circuits for high average power, millimeter-wave applications. This potential for cost reduction occurs because the conductor arrays, or ladders, can be constructed from photo etched (chemically milled) or electron beam milled material. This creates circuits in which there is less likelihood of tolerance buildup and for which there are relatively few parts.

1.2 SYNOPSIS OF PREVIOUS WORK

Related work has been done on NASA Lewis Research Center contracts NAS-3-21930, NAS-3-22445, NAS-3-22466 and NAS-3-23259. On these programs, tubes were designed for operation at both 29 GHz and 39.5 GHz at CW power levels in excess of 200 W. A tube was successfully built and tested at 29 GHz, and the present contract includes further design, fabrication, and testing of tubes at that frequency.

Initially work centered on the development of an appropriate circuit. These original circuit designs were cold tested in scale model versions,[2] which resulted in the present circuit configuration. (Further elaboration of the circuit design is given in Section 2.1.)

1.3 SUMMARY

Section 2.0 presents a history of the TunneLadder design and a synopsis of the circuit design approach used on this program. This section also presents an overview of the work done on earlier programs.

Section 3.0 describes the electrical design and design modifications. Most of the circuit dimensions related to transmission line and beam-wave interaction behavior are well established, but some circuit dimensions were modified to improve the frequency response. The most extensive modifications were done on the collector, which was modified for high efficiency performance. The cathode-anode spacing was also changed slightly to improve the beam transmission.

Section 4.0 outlines the approach taken to make the vacuum assembly less likely to leak, more rugged, and easier to assemble. This approach, derived from the 39.5 GHz TunneLadder, was modified to conform to constraints dictated by the magnet structure, and to a desire to maintain existing mechanical design for standard subassemblies.

Section 5.0 discusses the assemblies built during this program and includes pictures of several such assemblies.

Section 6.0 describes the testing done on VTA-6298A1, S/N 102 the results of those tests, and the conclusions drawn from those results.

Section 7.0 presents the conclusions reached as a result of the work reported; and, on the basis of those conclusions, Section 8.0 offers recommendations for appropriate extensions of this work.

2.0 HISTORY

2.1 BACKGROUND

In the early 1950s, the thin, flat ladder was recognized as a practical periodic element at millimeter wavelengths, provided one could invent a slow-wave interaction circuit incorporating it.[3,4]

The first ladder-based slow-wave circuit studied was a plain, rectangular waveguide with the ladder installed in the broad wall. The rung span was less than the waveguide breadth.[5] Slow-wave propagation was achieved over a useful bandwidth extending downward from the half-wave resonance frequency of the rung. The bandwidth became greater when a ridge was introduced within the waveguide.[6] The propagation was "forward wave", and the bandwidth depended on both the ridge-to-ladder capacitance and the space available for loops of rf magnetic field to expand beyond the rung anchor points.

During this period and beyond, a single ridge plus a thin, flat ladder combination appeared in low-voltage tubes – primarily backward-wave oscillators (BWOs) for frequencies up to 300 GHz.[7-9] In these designs, the disposition of metal around the rung anchor points varied;[10] hence the bandwidth contribution relative to that from the ladder-to-ridge capacitance was not constant.[11] The present emphasis on higher power levels requires that the rungs be anchored directly and perpendicular to flat, solid walls to maximize rung cooling;[12] consequently, the bandwidth must be determined solely by the ridge capacitance. Most analytic efforts to model the structure's field and impedances stipulated extensive flat walls normal to the array of rungs.[12-15] Beam voltages of at most a few kilovolts were characteristic of millimeter-wave tubes in the 1950s and early 1960s, so in order to avoid an unreasonably fine ladder pitch, only space-harmonic interaction was considered at these low beam velocities. The beam-wave phase shift per period was between π and 2π for a BWO and between 2π and 3π for an amplifier. Thus the first point made in H.G. Kosmahl's 1978 presentation was that the tens-of-kV beam voltages favored today would permit non-space-harmonic operation at millimeter wavelengths of a "forward-wave" ladder-based amplifier with a relatively coarse pitch.[16]

"Fundamental/forward" TWT interaction implies per se a relatively high gain/inch, but Kosmahl's second point was that the gain rate would benefit further from the high interaction impedance associated with the ladder. This impedance is due, in part, to the rung resonance at a frequency close to the operating frequency and the consequent high dispersion and low group velocities. These properties also predict a rather narrow "hot" bandwidth which might, however, be acceptable for certain applications.

The principles stated above led to the previous study and development programs[17] and to the present program. In the study program, before TWT designs that were practical embodiments of Kosmahl's principles were devised and evaluated, some cold-test experimentation was done with an intentionally simplified slow-wave structure. These experiments showed the effects of dimensional changes in a geometry featuring the basic structural elements – rungs, ridge, and side walls (see Figure 1). Other tests included measurements of the effects of double ridges on the ω-β curve and on the interaction impedance.

The move from the earlier space-harmonic and low-power approaches to the forward/fundamental approach and high power for millimeter wavelengths created a very different physical situation. Beam power densities on the order of a few MW/cm^2 were necessary, and pencil-beam optics were the only means for making these power levels manageable from the viewpoint of both the gun and the interaction structure. On the interaction structure side, a low percentage interception was consistent with having a pencil beam in a round "tunnel". On the gun side, a conventional axisymmetric gun, sufficiently convergent to avoid undue cathode loading, permitted the requisite 100 A/cm^2 or more of beam current.

The simple ladder-plus-ridge design is shown at the left in Figure 1. The ladder is then formed and doubled to allow the passage of a pencil beam; and thermal anchoring to dielectric posts increases the thermal capacity for handling beam interception. The forming of the ladder produces a noncircular tunnel for the beam. This design provides thermal paths through the dielectric posts to the ridges for beam-interception heating, localized where the rungs are closest to the beam. RF heating in the rungs occurs mainly near the side walls where there is a direct connection.

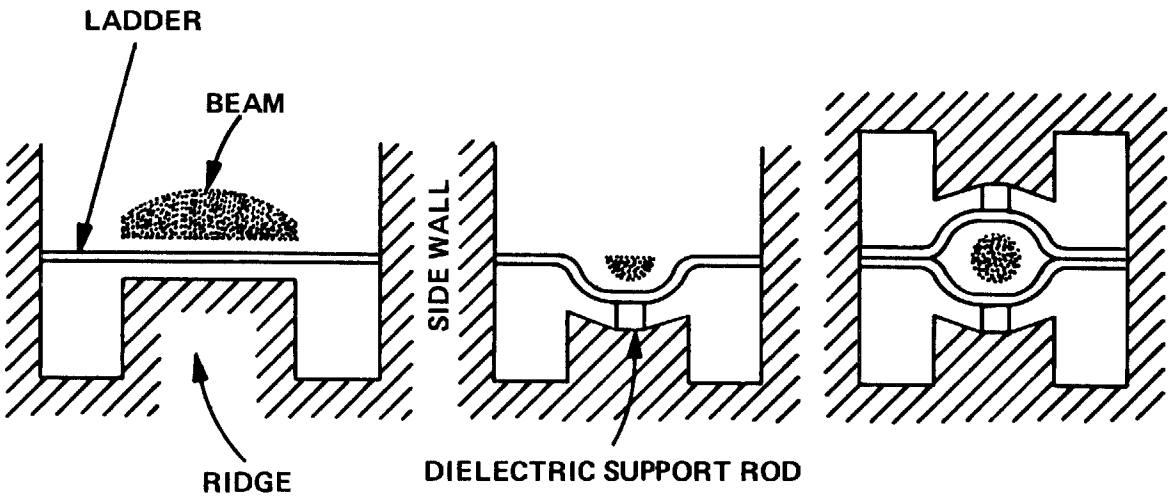

FIGURE 1. FLAT SINGLE LADDER TO "TUNNELADDER" DESIGN

These ideas underlay the basic "TunneLadder" interaction structure at the right in Figure 1 with two ridges and a ladder assembled from two identical components. As stated before, the shaping of the ladder halves provides a more or less oval beam tunnel (with the beam interception occurring primarily at the two positions where heat travels directly outward through the dielectric support rods). The double-ridge system then permits propagation of a mode which is TE at the lowest propagating frequency and whose fields are antisymmetric with respect to the ladder – in addition to the desired mode which is similarly TE-derived but symmetric with respect to the ladder. With the new ladder-half shaping, the passband upper edge for the desired (symmetric) mode is lower than if the rungs were straight, requiring an inward adjustment of the enclosure side walls. However, the passband upper edge for the antisymmetric mode is considerably higher – by the ratio of the total rung length to half the circumference of the tunnel.

The dielectric supports proposed are of high thermal-conductivity Type IIA diamond with a rectangular cross section of 0.2 mm (0.008") by 0.38 mm (0.015"). The copper of the ladder rungs and ridges is zirconium doped to effect a strong thermocompression bond to the diamond without risk of contaminating nearby exposed diamond surfaces. Details relating to these supports and the bonding are given in Section 4.0. The information in this section and Section 3.1 is also presented in almost the same form in an earlier report.[18]

2.2 RECENT WORK

From 1981 to 1984, the circuit described above was reduced to practice. A 29 GHz TWT was designed, and two tubes were built and tested. (The circuit design and cold test are described in Section 3.0.) The basic design approach is sound, as demonstrated by the performance of the two tubes, as shown in Figures 2 through 7.

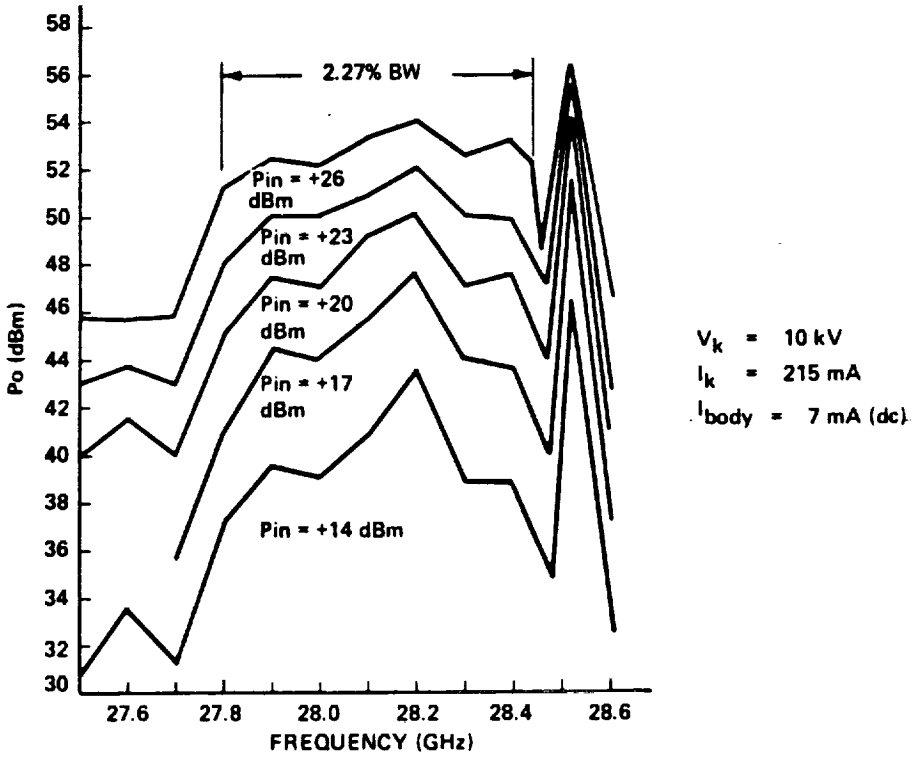

FIGURE 2. POWER OUTPUT vs FREQUENCY FOR DIFFERENT INPUT DRIVES, S/N 101

D1056
F580

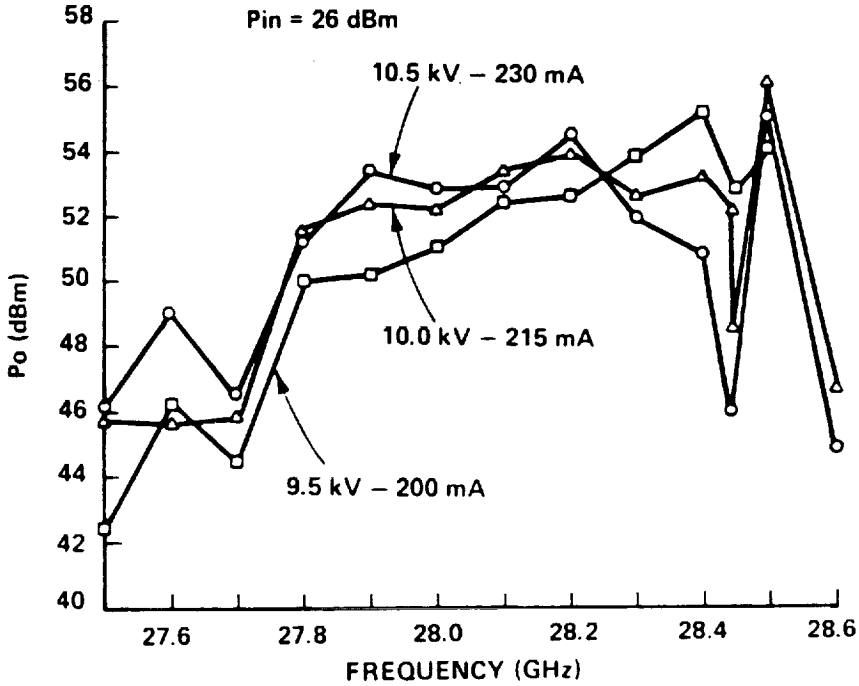

FIGURE 3. EFFECT OF VOLTAGE TUNING ON OUTPUT POWER vs FREQUENCY, S/N 101

D1057
F580

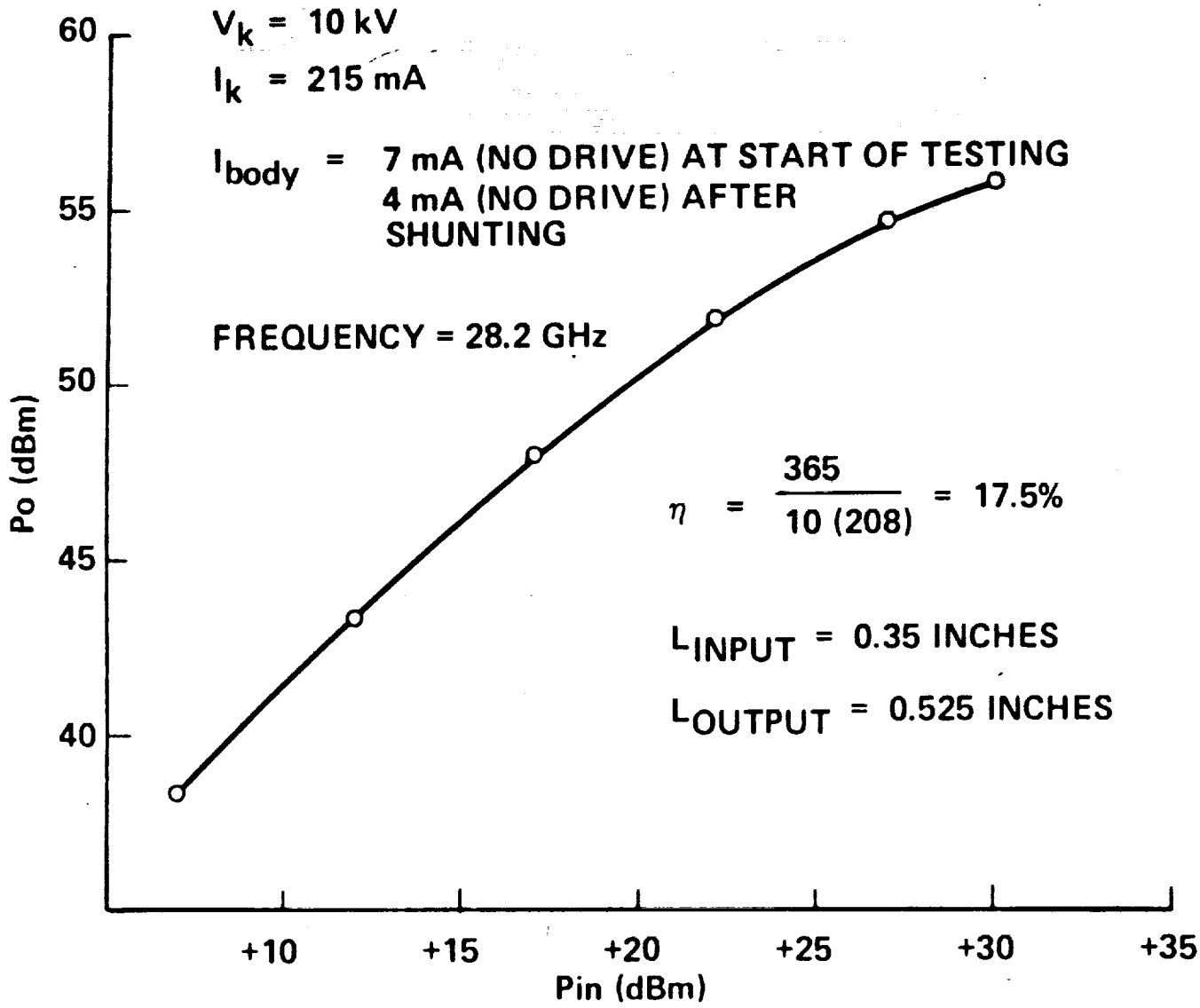

FIGURE 4. OUTPUT POWER vs INPUT DRIVE, S/N 101

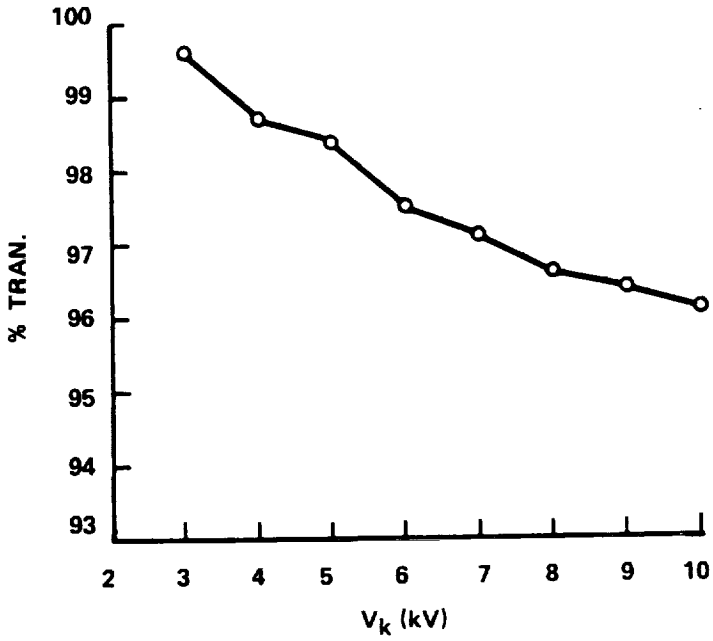

FIGURE 42. BEAM TRANSMISSION FOR S/N 102

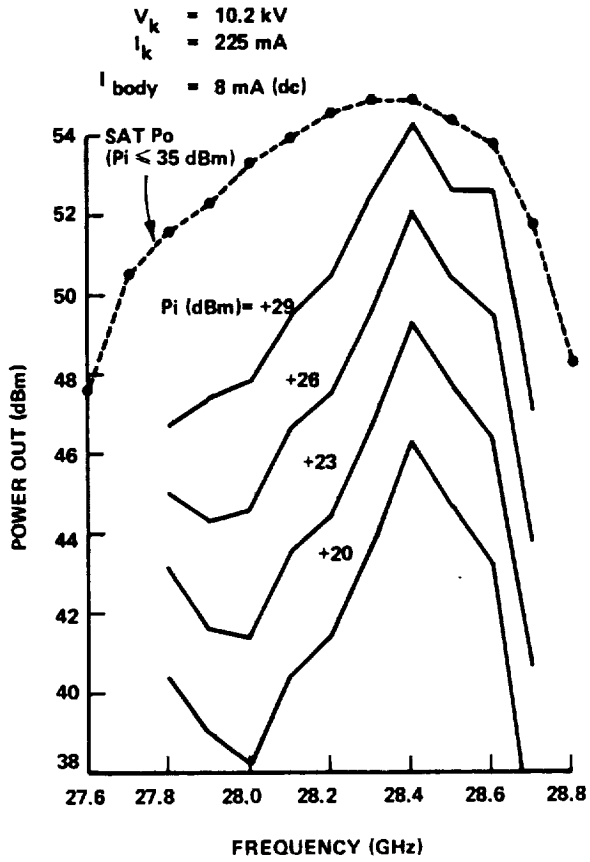

FIGURE 5. POWER OUTPUT vs FREQUENCY FOR DIFFERENT INPUT DRIVES, S/N 102

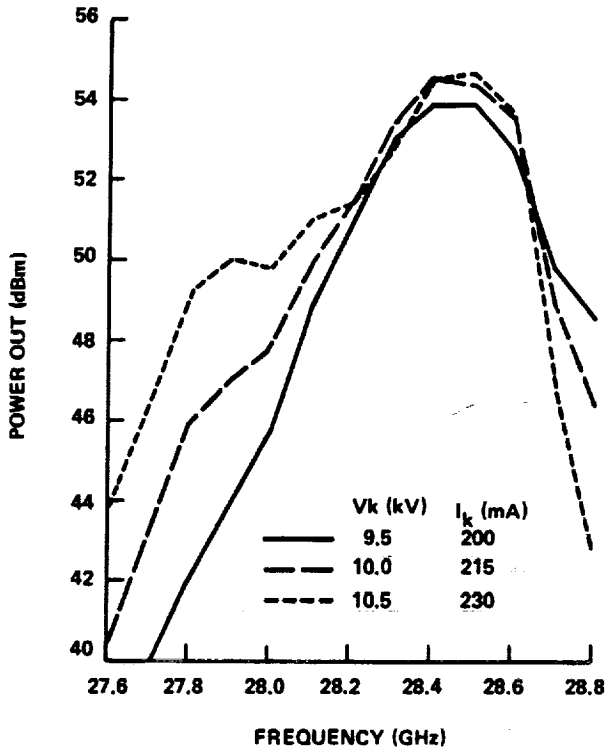

FIGURE 6. EFFECT OF VOLTAGE TUNING ON OUTPUT POWER vs FREQUENCY, S/N 102

D1060
F580

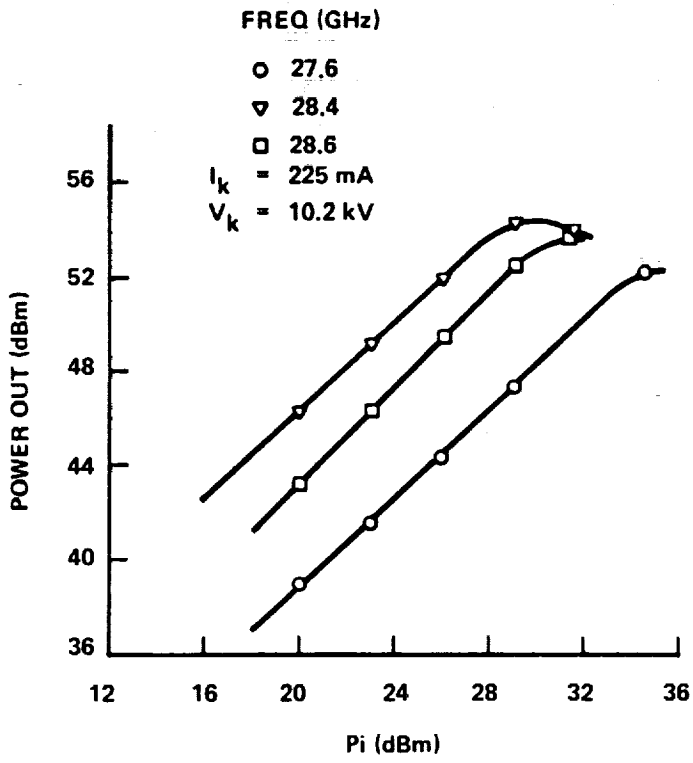

FIGURE 7. OUTPUT POWER vs INPUT DRIVE, S/N 102

D1061
F580

3.0 ELECTRICAL DESIGN

This section describes the technical methods used to predict electrical performance. These methods were proved in the previous program. The cold-test work which defined the circuits and the circuit designs themselves are discussed in Section 3.1, and the method by which the circuit is matched to the waveguide is described in Section 3.2. Section 3.3 discusses the window designs, including the modification undertaken to reduce the likelihood of inband window resonance modes. Section 3.4 contains a brief description of the gun developed in earlier programs. The multistage depressed collector designed on this program is described in Section 3.5, and a brief presentation of the previously designed magnet structure is given in Section 3.6.

3.1 CIRCUIT DESIGN

3.1.1 Cold-Test Experiments

The actual circuit design resulted from cold-test experiments with a 10-times scaled model of a 29 GHz circuit whose geometry was determined from the results of NASA Contract 3-21930.

The first scale model used Stycast to represent the diamond cubes and machined copper for the chemically milled Amzirc ladders. The outer surfaces of the cold-test model were aluminum, and parts of the waveguide sidewalls were movable to establish the frequency band. The sidewall dimensions were the same in the final waveguide design to simplify parts and subassembly fabrication. The ω-β diagram for a typical TunneLadder circuit is shown in Figure 8.

Tests included varying the diamond-cube width and the ridged-waveguide wall spacing; the results shown in Figure 9 established the circuit dimensions for the tubes of this program. The half-structure drawing of Figure 10 gives the 10X-scaled dimensions. The ω-β and perturbation data obtained in cold test were used in the small- and large-signal programs to establish tube performance with coputer-predicted data shown in Figure 11.

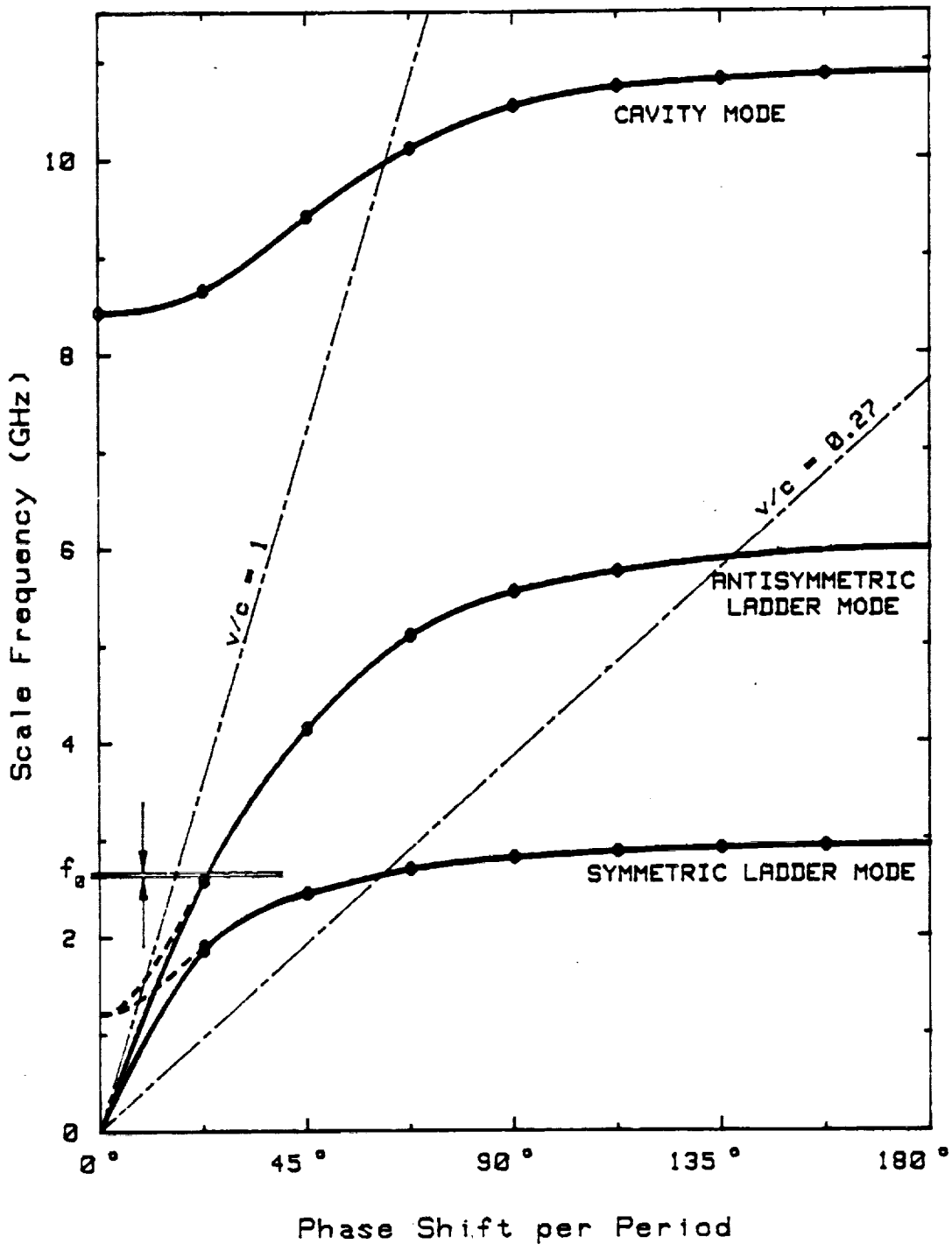

FIGURE 8. ω - β DIAGRAM FOR TYPICAL "TUNNELADDER" CIRCUIT

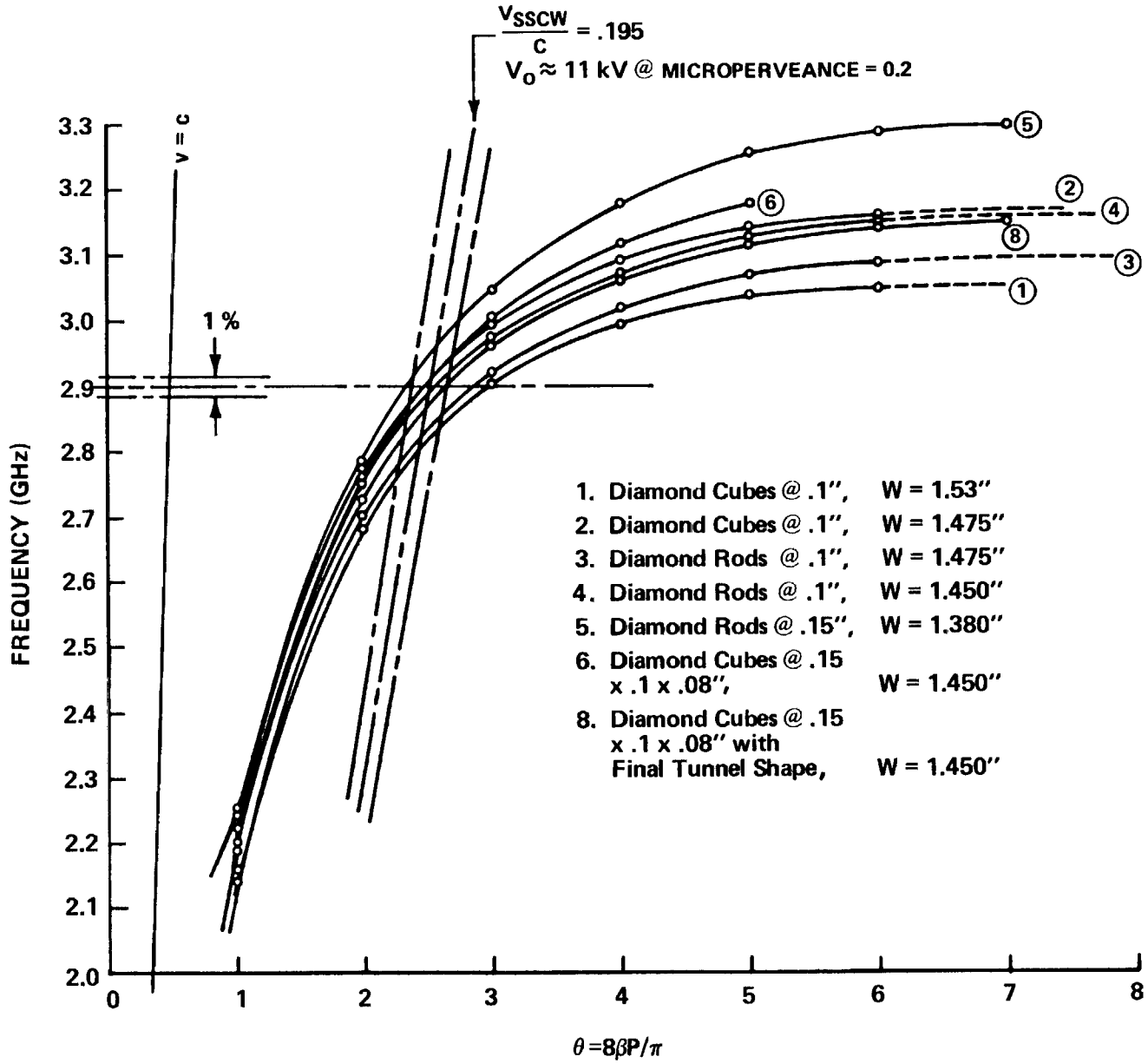

FIGURE 9. CIRCUIT COLD-TEST RESULTS

D1063
F580

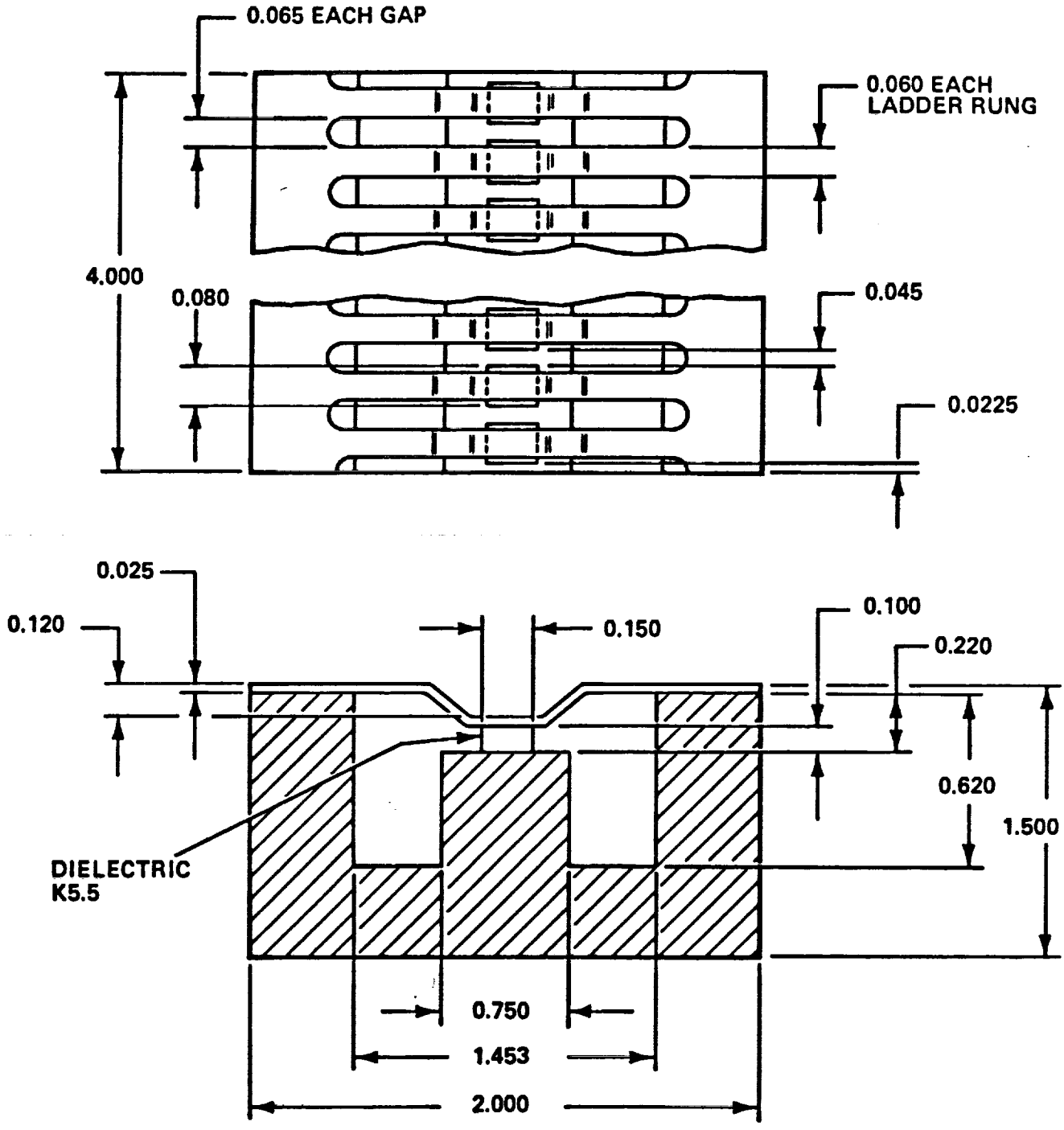

FIGURE 10. HALF OF THE FINAL SCALED COLD-TEST MODEL

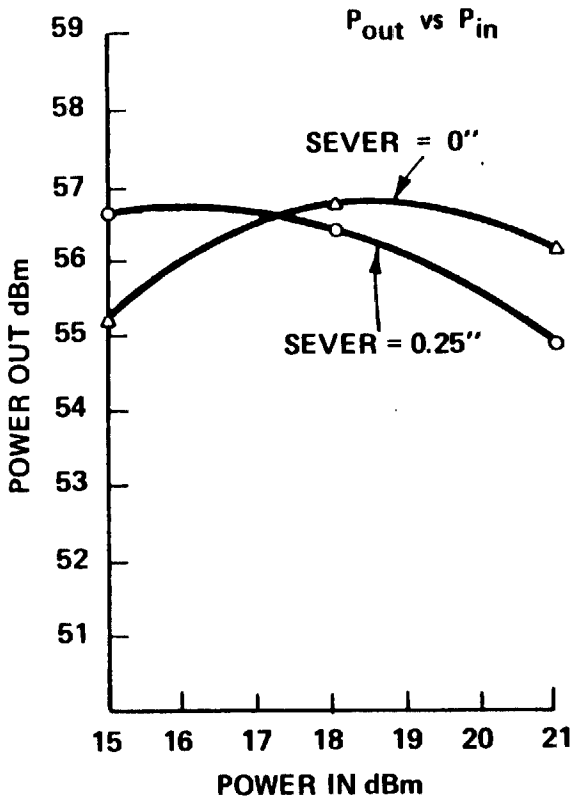

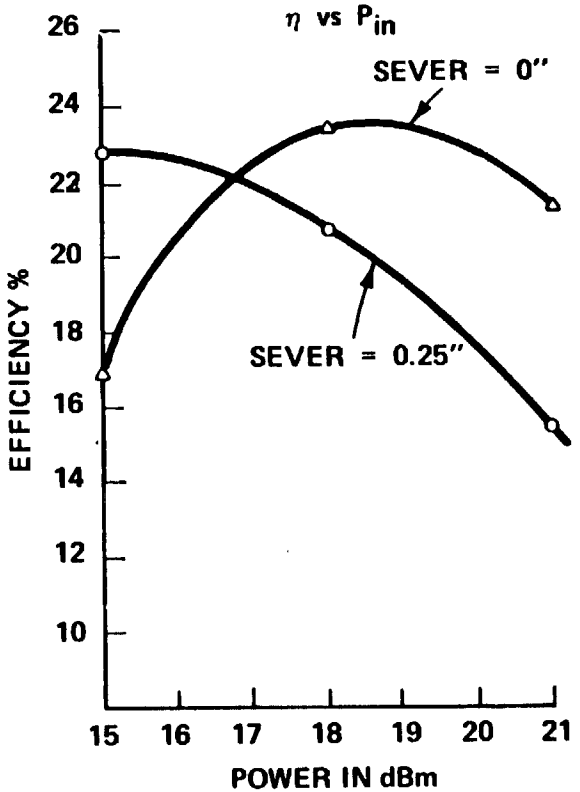

F	=	2.9 GHz	C	=	0.1027
V_o	=	10 kV	B	=	0.533
I_o	=	0.20 A	d	=	0.055
			QC	=	0.039
			γb	=	0.743
			b/a	=	0.601
			Rw	=	0.381

INPUT SECTION – 28 PERIODS

OUTPUT SECTION – 42 PERIODS

v/c	=	0.1843	BOTH SECTIONS
Z_{AXIS}	=	168.3 Ω	
LOSS	=	0.387 dB/IN	

13 dB GAIN IN INPUT SECTION

FIGURE 11. COMPUTER-PREDICTED PERFORMANCE

D1065
F580

After the circuit design was completed, the cold-test effort concentrated on the waveguide/circuit transition. The 10X-scaled circuit model of Figure 12 is shown with the scaled waveguide-transition model in Figure 13. The final cold-test coupler design, shown in Figure 14, includes the dimensions of the coupler tuning elements: inductive iris, capacitive post, and reduced-height waveguide short. Figure 15 shows the cold test results obtained by using these optimized dimensions.

The coupler VSWR is better than 1.6:1 over a 5 percent bandwidth and better than 2:1 over 10%. This is more than satisfactory for the expected 1 to 3 percent "hot" bandwidth. It should be possible to achieve a maximum VSWR better than 2:1 for the actual 29 GHz circuit, even with the double-ended matched circuit implemented in the first models. The only other cold-test experiments were undertaken after later work showed that the diamond cubes needed metallized caps to accomplish brazing to the Amzirc ladder rungs. These tests forecast a 2 to 5 percent lowering of the operating frequency band, later verified in actual tube tests. The changes to the circuit design necessary to move the operating frequency band back to 29 GHz involved a shortening of the ladder rungs and a corresponding decrease in the width of the double-ridge waveguide halves. This was accomplished with a machining change in the circuit half blocks alone and no changes in any of the assembly fixtures.

3.1.2 Actual Size RF Circuit Design

The end of Section 2.1 contains a brief description of the key elements in the construction of the rf interaction structure. Two shaped ladder elements were made by chemical milling, each supported by Type IIA diamond cubes brazed to half of a double-ridge waveguide. These symmetrical halves were mated, forming the TunneLadder circuit. All brazes were made using Amzirc alloy for active brazes. Amzirc is a copper alloy doped with zirconium, which makes active-metal brazing possible. During the course of this program it became clear that the active metal braze alone was not sufficient to provide a reliable bond. Therefore, gold foil was brazed onto each joint to provide a diffusion bond as well.

The most critical components in the actual-size fabrication of the circuits were the shaped and chemically milled Amzirc ladder elements. These elements were satisfactorily manufactured by Elcon, Inc., of San Jose, CA. The tolerance on individual rung and gap dimensions was held to within ±0.005 mm (0.0002"). The total ladder length was

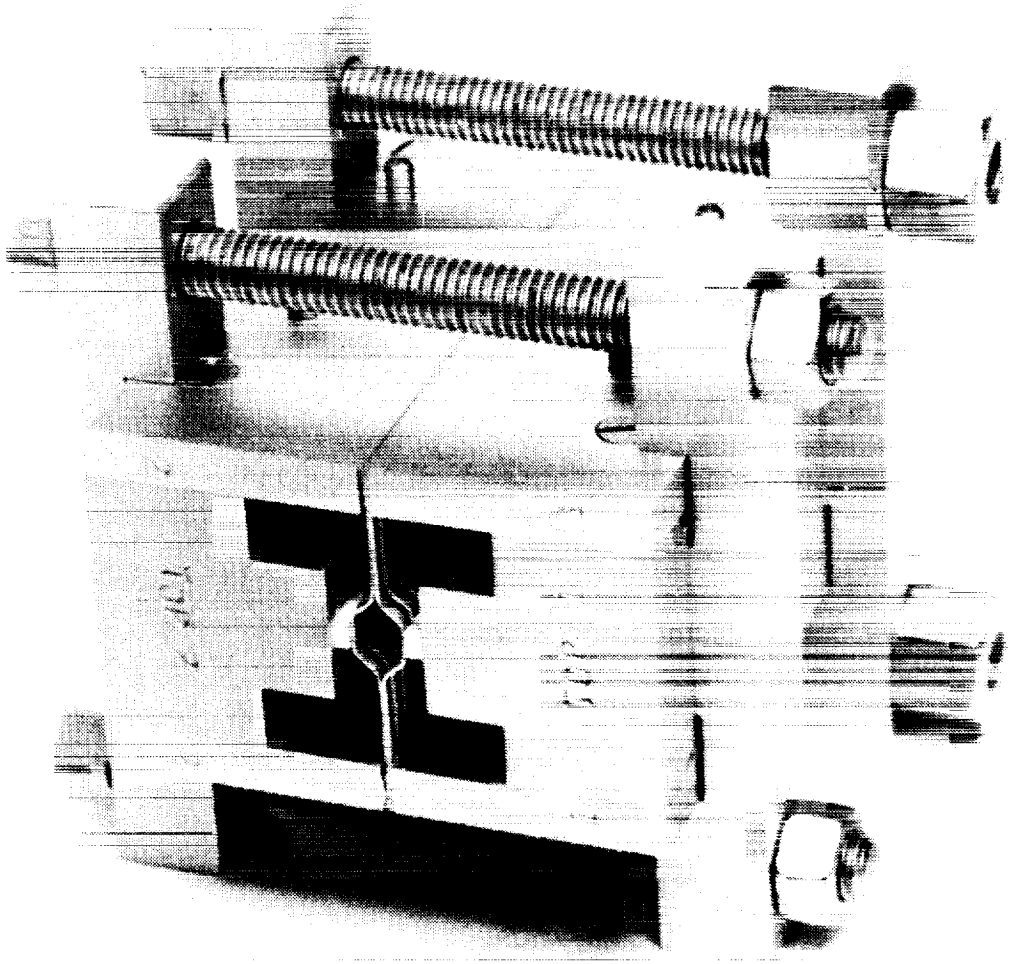

F580

FIGURE 12. 29 GNz/10 kV TUNNELADDER CIRCUIT GEOMETRY – IN 10X COLD-TEST SCALE MODEL (DIAMONDS SIMULATED BY STYCAST BLOCKS)

FIGURE 13. 10X COLD-TEST MODEL FOR DEVELOPING WAVEGUIDE TRANSITION

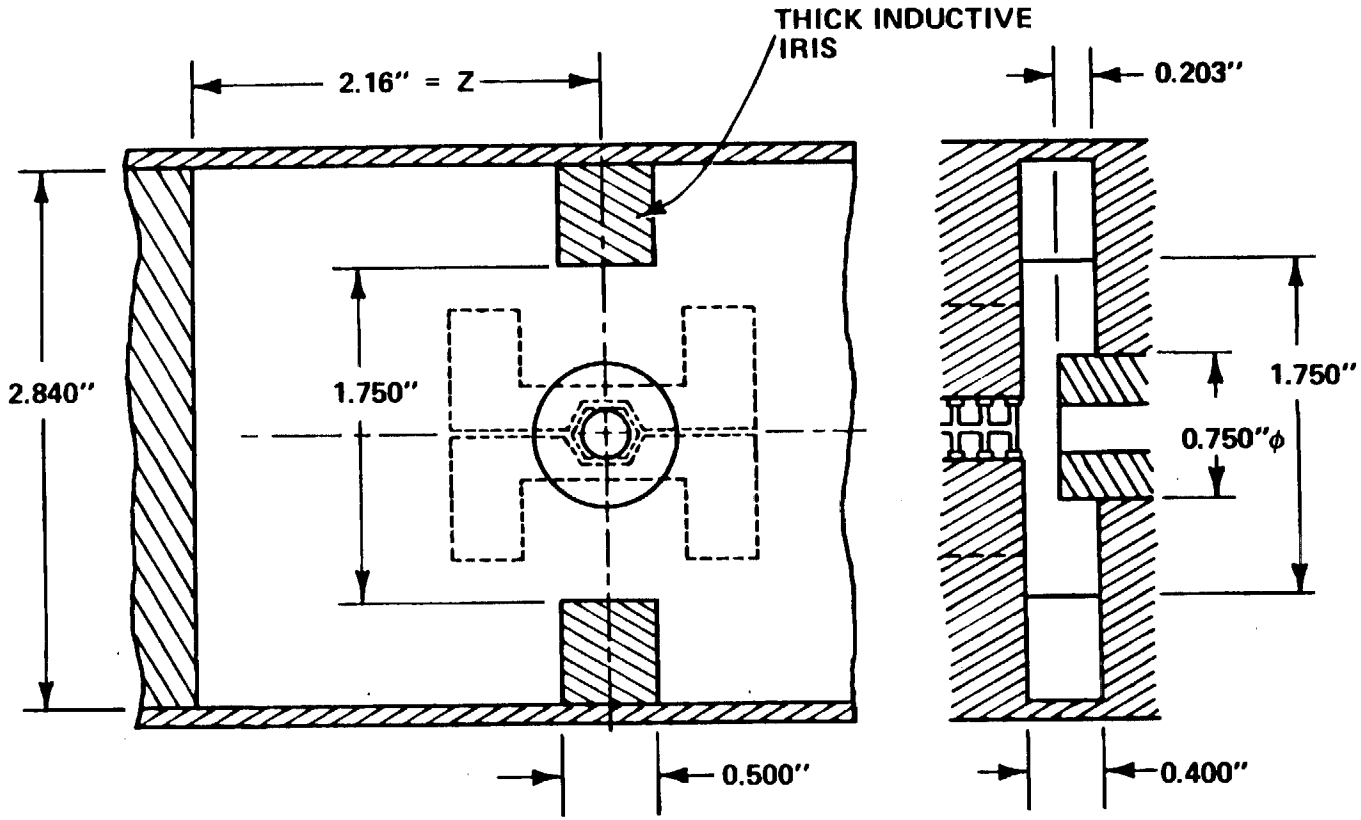

FIGURE 14. CIRCUIT/WAVEGUIDE COUPLER DESIGN (10 X SCALE)

D1068
F580

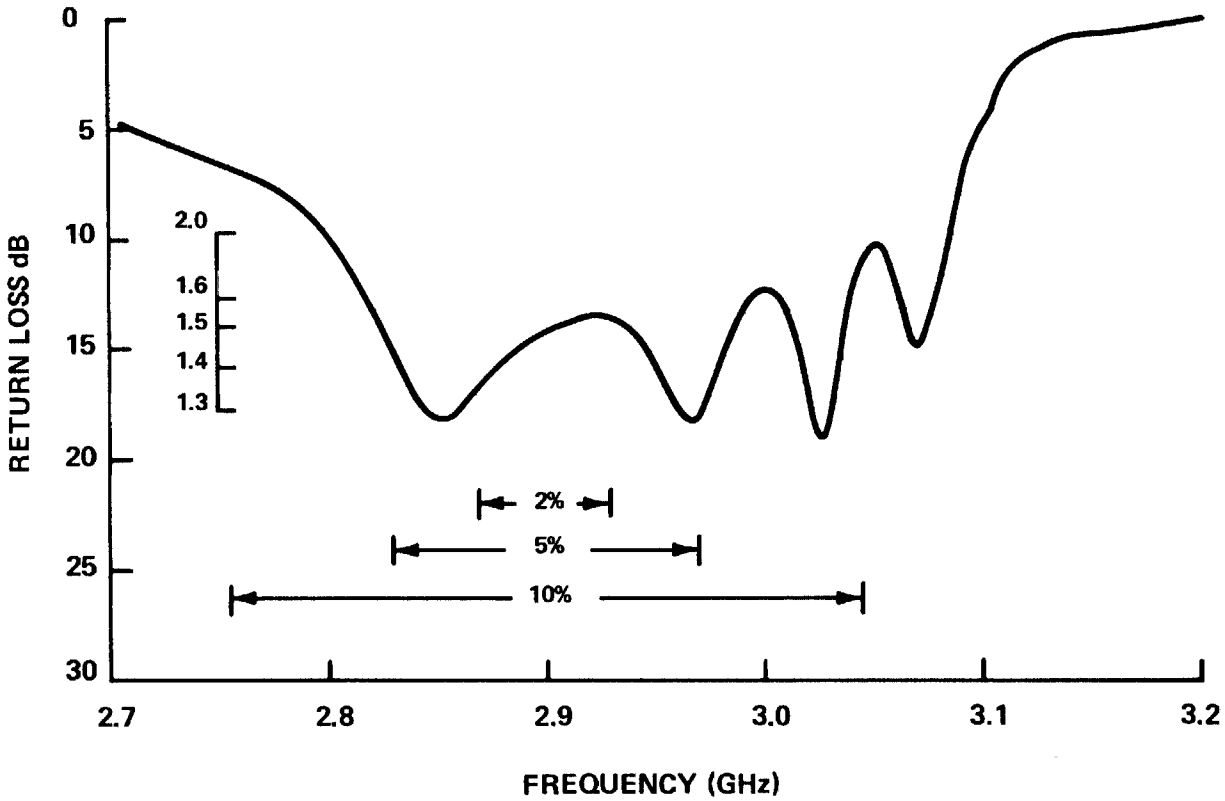

FIGURE 15. COLD TEST WAVEGUIDE TRANSITION MATCH

D1069
F580

controlled to prevent an "accumulation of tolerances" of the individual rungs and gaps. The gold thickness is 0.0635 mm (0.0025") with the rungs 0.152 mm (0.006") wide at a pitch of 0.318 mm (0.0125").

The most critical procedure on which the circuit design depends is the brazing of the diamond cubes to the waveguide ridge. The diamond cubes, each 0.3 ±0.001 by 0.38 ±0.02 by 0.2 ±0.02 mm, were brazed onto each waveguide ridge with the aid of a chemically milled alignment fixture. Diamond was used because of its superior thermal conductivity. Figure 16 compares diamonds thermally with other insulators and conductors. At room temperature, Type IIA diamond as a thermal conductor is almost an order of magnitude better than copper, which is only slightly behind silver as the best metal conductor. A technique was needed to braze the diamond cubes to the copper ridge. For this purpose, the top surface of the ridge itself was made of Amzirc, and special fixtures were designed to provide the necessary interface pressures. The procedure evolved through several stages with the final fixture design maintaining uniform pressure at the interfaces during the braze cycle.

We have assumed that once the technology was developed to braze the diamond cubes to the waveguide ridge, it could be applied directly to the brazing of the diamond cubes to the Amzirc ladder rungs. This was not the case. Early tests showed that the pressure necessary to achieve the active diffusion braze flattened and widened the ladder rungs so that they extended beyond the mating face of the diamond cube. To eliminate the excess pressure, the gold-diffusion braze was substituted. First, a technique was developed to metallize the top face of each diamond cube with Amzirc and gold. The ladder rungs were then sintered to the metallized diamond cubes by a gold diffusion braze with a minimum of pressure.

The next step was to machine the waveguide half blocks before brazing two of them into a complete TunneLadder assembly. The process involved the design and fabrication of three fixtures to protect and align the circuit halves during the machining operation. The end result was a machined half circuit section, ready to be brazed to its mate, and both ready to be brazed to the input/output waveguide transitions and the cooling-block subassemblies.

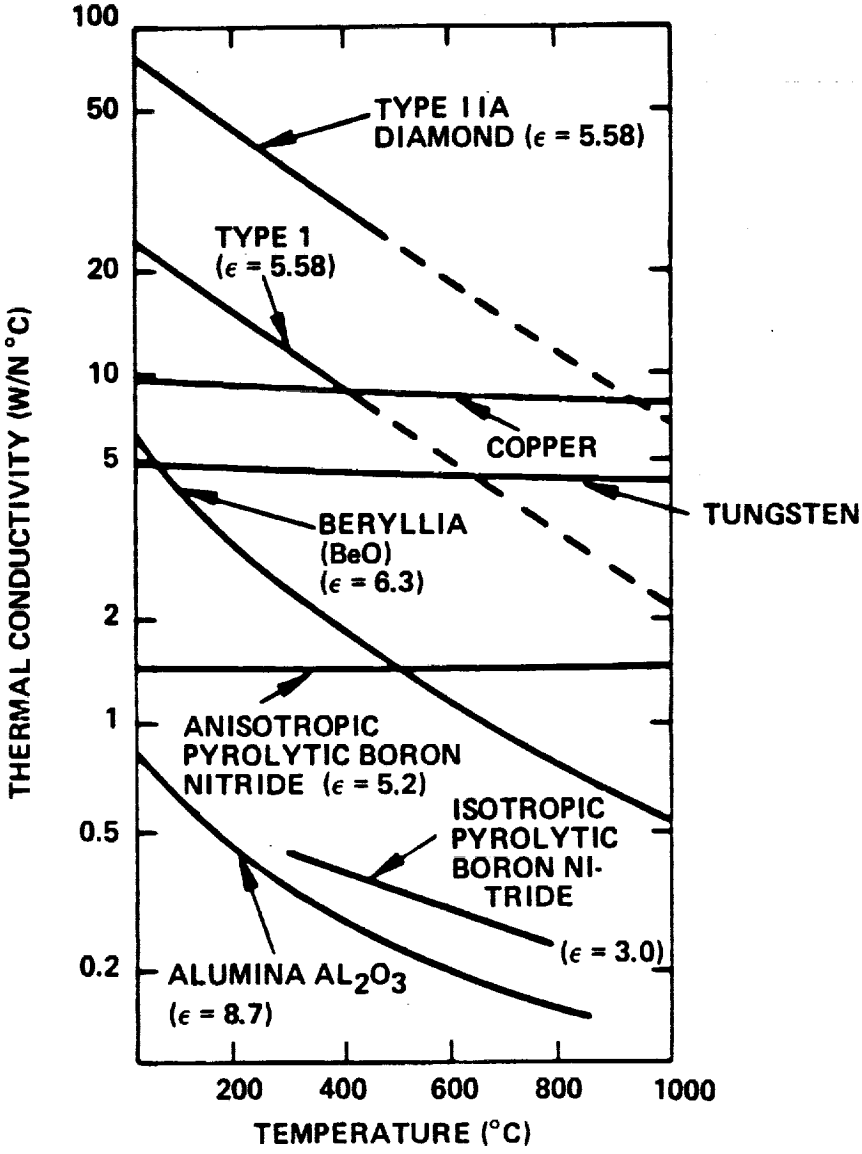

FIGURE 16. THERMAL CONDUCTIVITIES OF MATERIALS AS A FUNCTION OF TEMPERATURE

Brazing details for rf circuit fabrication are shown in Figures 17-20. Figure 17 shows the brazing of an Amzirc shim to the waveguide block and the subsequent machining to produce the capped ridge; it also shows the diamond-to-ridge braze. A detailed insert shows the braze fixture, a chemically milled diamond cube spacer and an additional strip of Amzirc foil (to ensure sufficient zirconium atoms at the interface). These are heated in helium to 800°C in the special temperature-compensated fixture. The last insert in Figure 17 shows the metallizing of the top of the diamond cubes. This is achieved with a gold-topped strip of Amzric foil and a special temperature-compensated fixture.

Figure 18 first shows the trimming and height-sizing operation required to prepare the diamond/ridge assembly for brazing to the ladder element. The ladder-to-diamond braze is also done at 800°C in helium with the graphite fixture shown. Figure 19 details the procedure for brazing diamond cubes to the ridge block. The machined ridge block, the spacer, and the fixtures are all designed to provide the necessary alignment and pressure. Figure 20 outlines the procedure for brazing the ladder element to the diamonds as well as the ridge block. Shown are the details of the ladder element, the ridge block, and the fixtures necessary to braze at 800°C in helium.

The brazed ladder-ridge block assembly is then machined. The blocks must be machined so that two of them match, rung to rung, over the total length of the circuit. The waveguide has to be machined to accommodate the circuit transition. The fixtures not only aid in the precise machining of the circuit halves, but also protect the delicate ladder structures from damage during the process.

Other techniques for fabricating the ladders have been considered, but not implemented. For example, a type of copper that has alumina dispersed through it has the thermal and electrical properties of copper, but greater structural strength. This material is called Glidcop. But on investigation, Glidcop was found to undergo a change in shape when brazed and is, therefore, not a suitable candidate for ladder material. Another technique considered was electron beam etching of the circuit shapes, an approach that may be less expensive than chemical milling. However, no appropriate vendor was found who could create the necessary shape and pattern for the ladders.

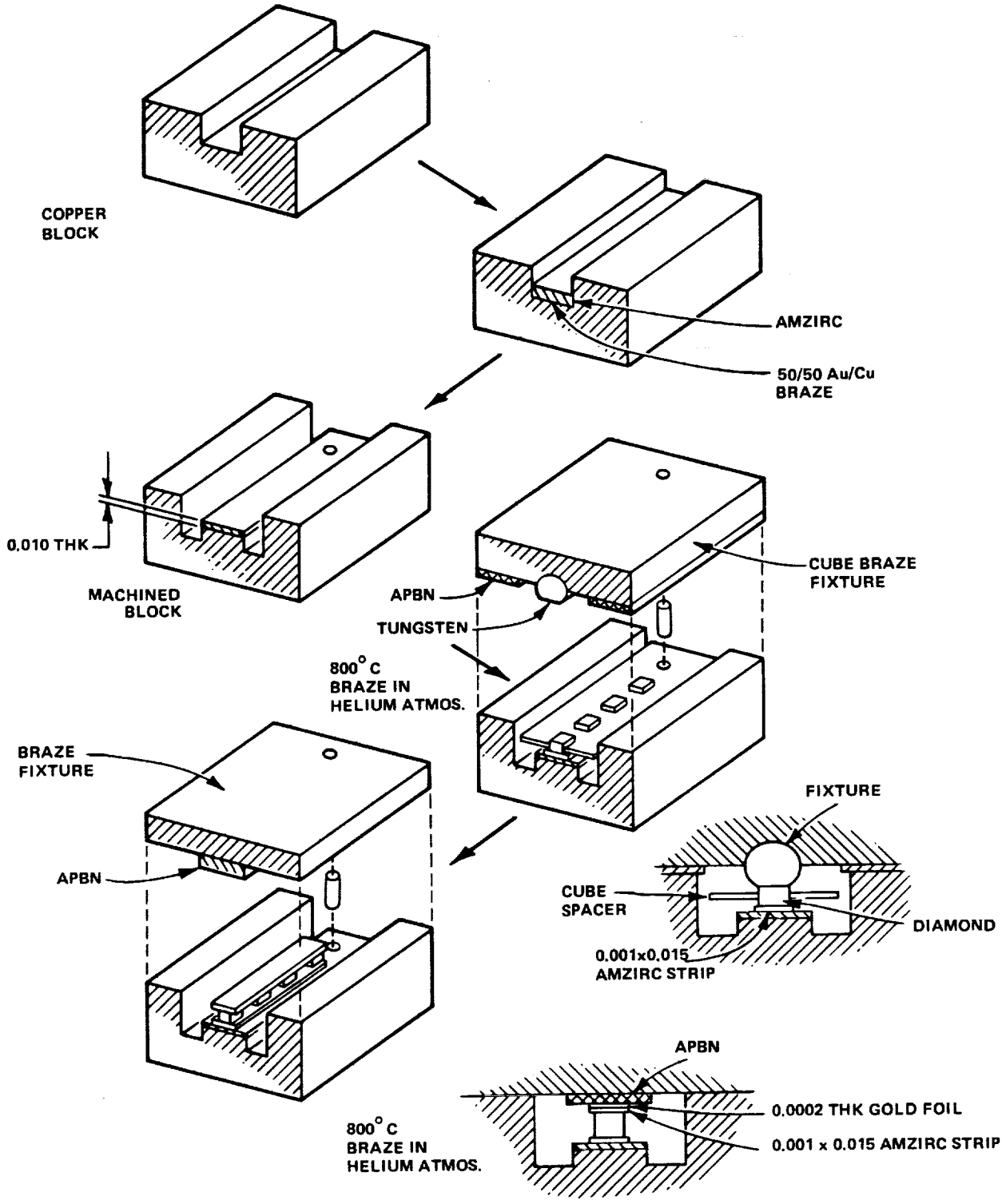

FIGURE 17. ASSEMBLY PROCEDURE THROUGH METALIZATION OF DIAMOND CUBES

D1071
F580

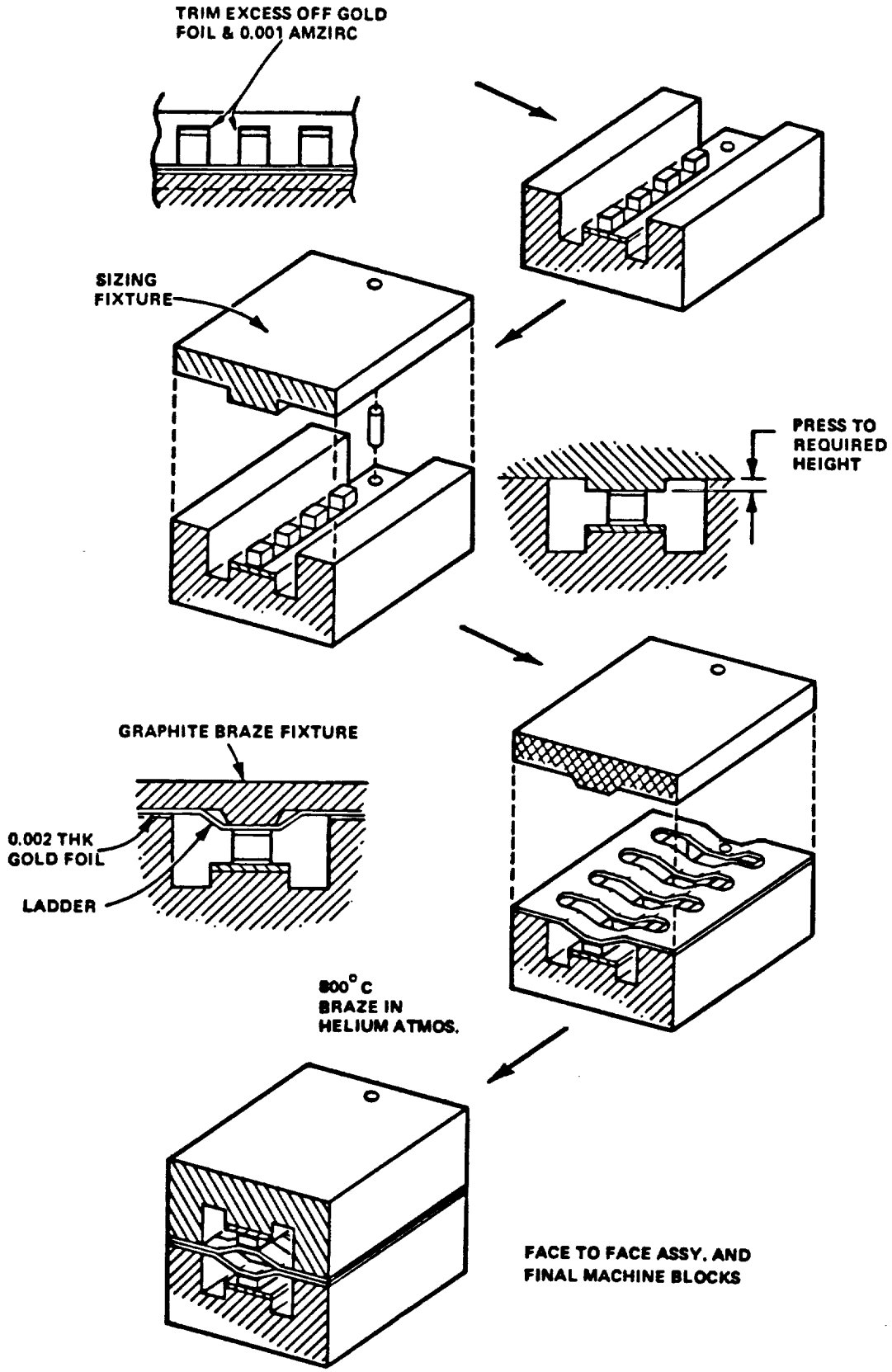

FIGURE 18. ASSEMBLY PROCEDURE THROUGH MATING OF THE TWO FINAL MACHINED HALVES.

D1072
F580

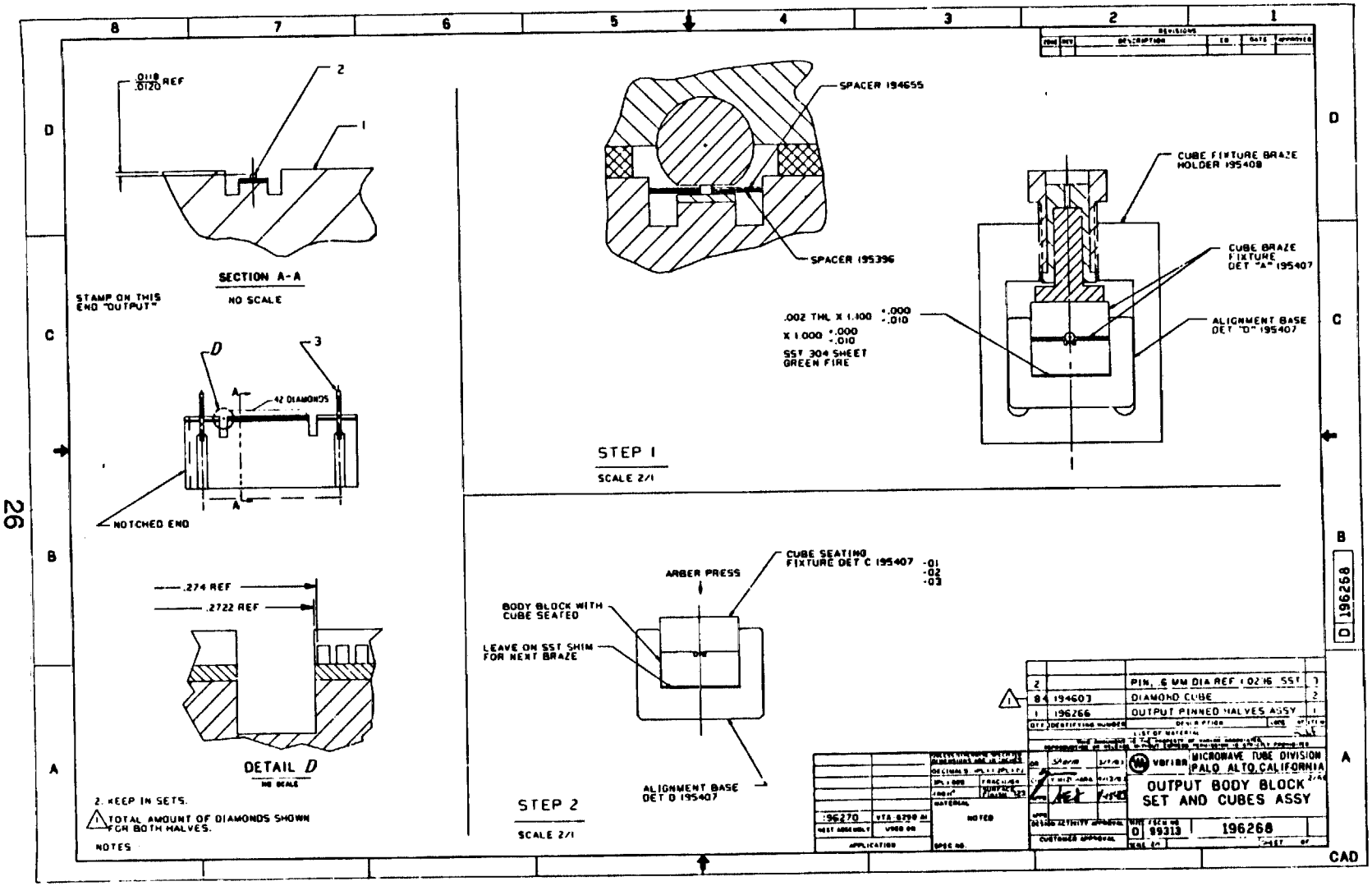

FIGURE 19. ASSEMBLY DRAWING OF DIAMOND BRAZE TO RIDGE ASSEMBLY

D1073
F580

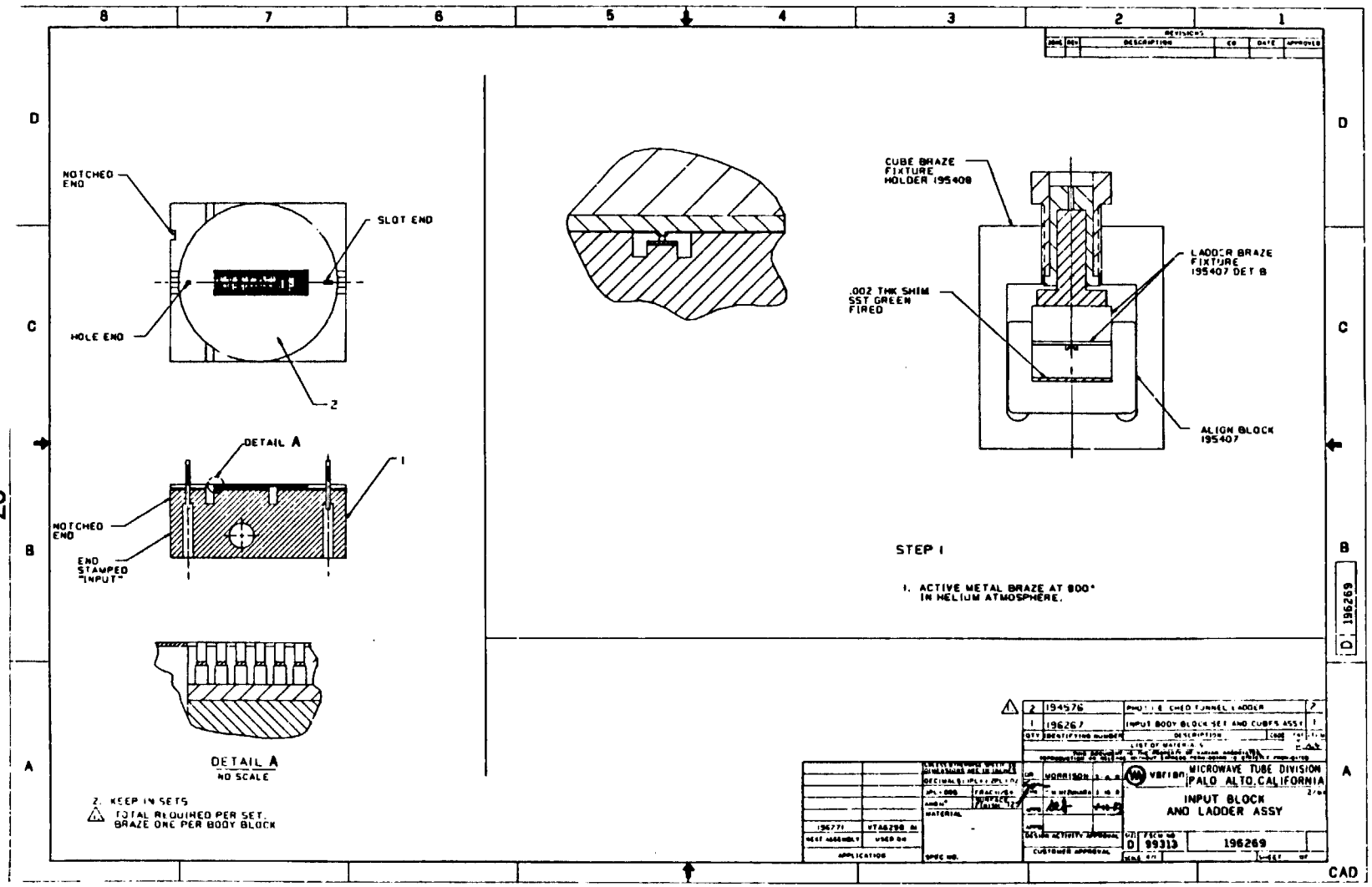

FIGURE 20. ASSEMBLY DRAWING OF BRAZE OF LADDER TO RIDGE–DIAMOND ASSEMBLY

D1074
F580

In summary, the circuit fabrication experiments led to the following observations and conclusions concerning copper/diamond bonds:

1. An active metal must be present; the zirconium content of Amzirc provides this.

2. The brazing atmosphere must be totally contaminant-free to prevent very weak bonds. Helium is used as it has fewer contaminants than are typical in "vacuum brazing".

3. The brazing temperature must be as low as possible to further minimize contamination risk; 800°C was selected.

4. All fixtures must be designed to avoid creating shear forces in the copper/diamond interface plane which provokes bond failure. Chemically milled copper fixtures are therefore used for spacing, and Type 304 stainless steel fixtures (whose expansion is the coefficient same as for copper to within 1 percent) are used for applying pressure to the diamond dice. (Although tungsten, with its ability to resist deformation under pressure, might be preferable, its thermal expansion coefficient is only about 24 percent that of copper, so the contraction difference on cooldown could break the diamond/copper bonds.)

5. Rung/diamond bonding must not cause ladder rung distortion. Given the small rung cross section, the pressure needed for true active metal bonding would indeed result in distortion. The technique is, therefore, supplemented by gold-diffusion bonding, which is also used to attach the ladder-rung ends to the enclosing cavity.

3.2 WAVEGUIDE DESIGN AND CIRCUIT HALVES

After the circuit halves are paired, machined, and brazed together, they are brazed to the waveguide transitions. Originally, these transitions were complex assemblies, and the brazing required another temperature-compensated fixture, complicated by the number of subassemblies in the ensemble yet like a "four port" version of the previous simpler fixtures. The redesigned circuit and waveguide transition combination, while complex, is much simpler than the earlier design and uses a simpler version of the braze fixture.

The input/output waveguide subassemblies each have a length of waveguide that tapers from normal height to reduced height. The inductive iris and capacitive post, placed at the point of transition to the circuit, are symmetrical to the beam axis. Several waveguide units have been brazed to machined TunneLadder blocks (which have been aligned rung to rung) by gold diffusion in helium at 800°C.

3.3 WINDOW DESIGN

Careful re-analysis of the window designs, using a mode identification computer program, indicated that there was a window resonance at approximately 28.4 GHz. While this resonance was not visible from cold-test results, its existence may help to explain the frequency response of S/N 101 (see Figures 2 and 3).

A slight modification of the circular waveguide section in which the window was located moved the mode out of the tube operating band. This change in performance was accomplished without altering the window ceramic.

3.4 GUN DESCRIPTION

The design of the Pierce gun was based on a low-frequency tube having a microperveance of 0.2 with a fairly high area convergence of 55. This gun was designed on the previous program and has been used on all three tubes. It was tested in the beam analyzer several times at various beam voltages to establish thermal velocity properties and actual projected beam size. The gun design, its high-voltage seal assembly, and the details of the electrode spacing are shown in Figure 21. The beam minimum occurs at 9.53 mm (0.375")

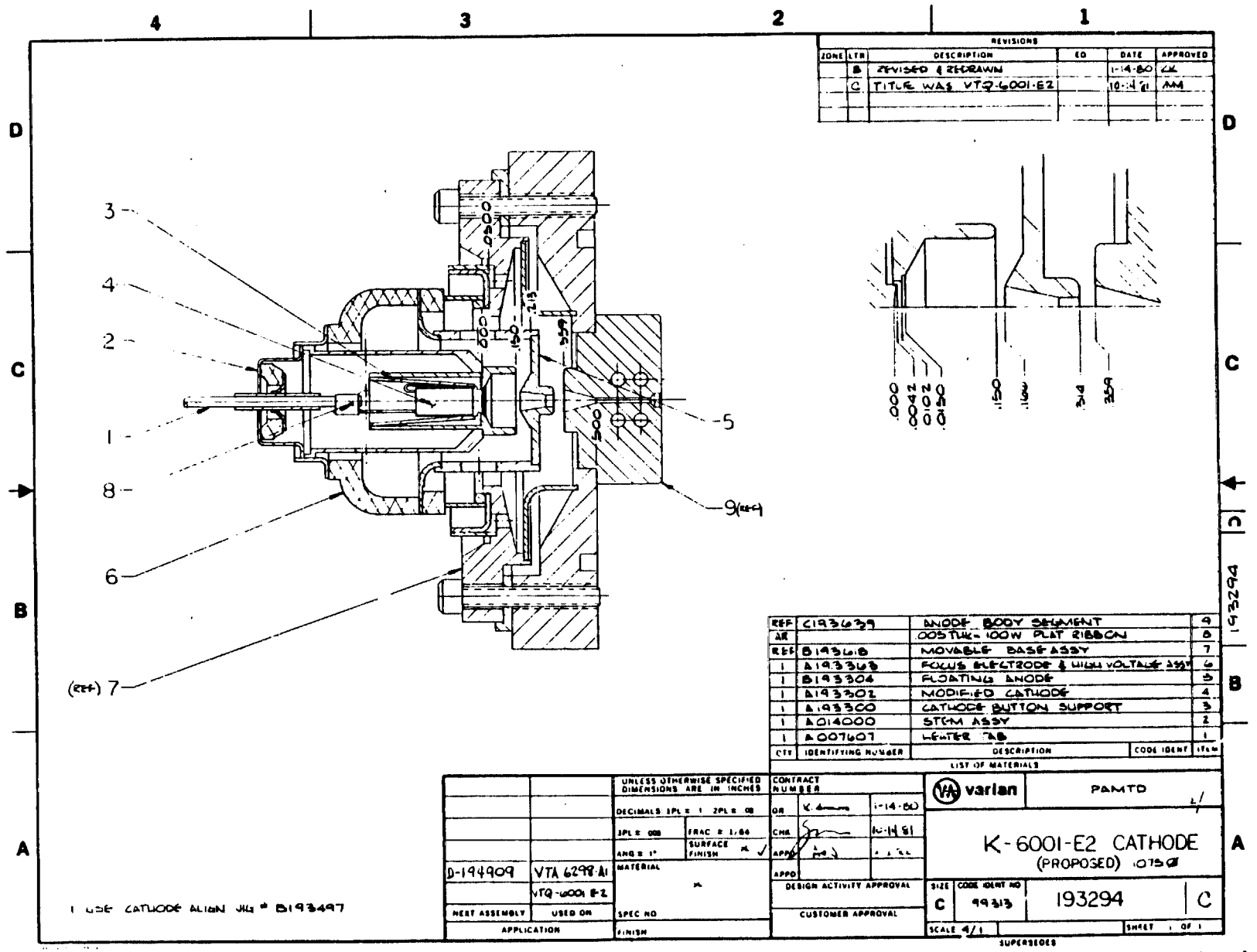

FIGURE 21. DETAIL OF GUN DESIGN

D1075
F580

from the cathode, at which point the beam has already been controlled by the magnetic field and will remain well controlled through the rest of the magnetic circuit – a fact confirmed by the excellent transmission achieved in the actual tubes. At 10 kV the electrostatic beam minimum diameter was 0.47 mm (0.0185") indicating a filling factor of 0.75, but with magnetic compression this value was reduced to 0.6 (0.38 mm or 0.015" diameter).

3.5 COLLECTOR DESIGN

A multistage depressed collector, designed for this tube type, is included in S/N 103. A cross section view of the collector is shown in Figure 22. The new collector consists of two stages biased at voltages between ground and cathode voltage, and a probe biased to the cathode voltage. The techniques used in designing this collector were similar to those used in designing multistage depressed collectors for helix type traveling-wave tubes. These tubes make extensive use of multistage depressed collectors to improve overall tube efficiency, both for energy savings and for a reduction in thermal stress.

The collector was designed using a computer program that analyzed the effects of various stage voltages and surface shapes on the collection of a spent beam. The spent beams used in these computations were intended to be characteristic of both no-drive and full-drive or saturation performance.

Another consideration that influenced this collector design was the desire to keep the beam constrained by the magnetic field until it was nearly at the entrance to the first stage of the collector. Because of the manner in which the tube is mounted in the magnet focusing assembly, the first collector stage is longer than normal. Nonetheless, a marked improvement in tube efficiency is likely. However, actual collector performance cannot be determined without testing on a tube.

3.6 FOCUSING DESIGN

The selected focusing system makes use of an existing permanent magnet composed of two radially magnetized $SmCo_5$ rings – one placed around the gun the the other around the collector. An iron casing completes the flux path.

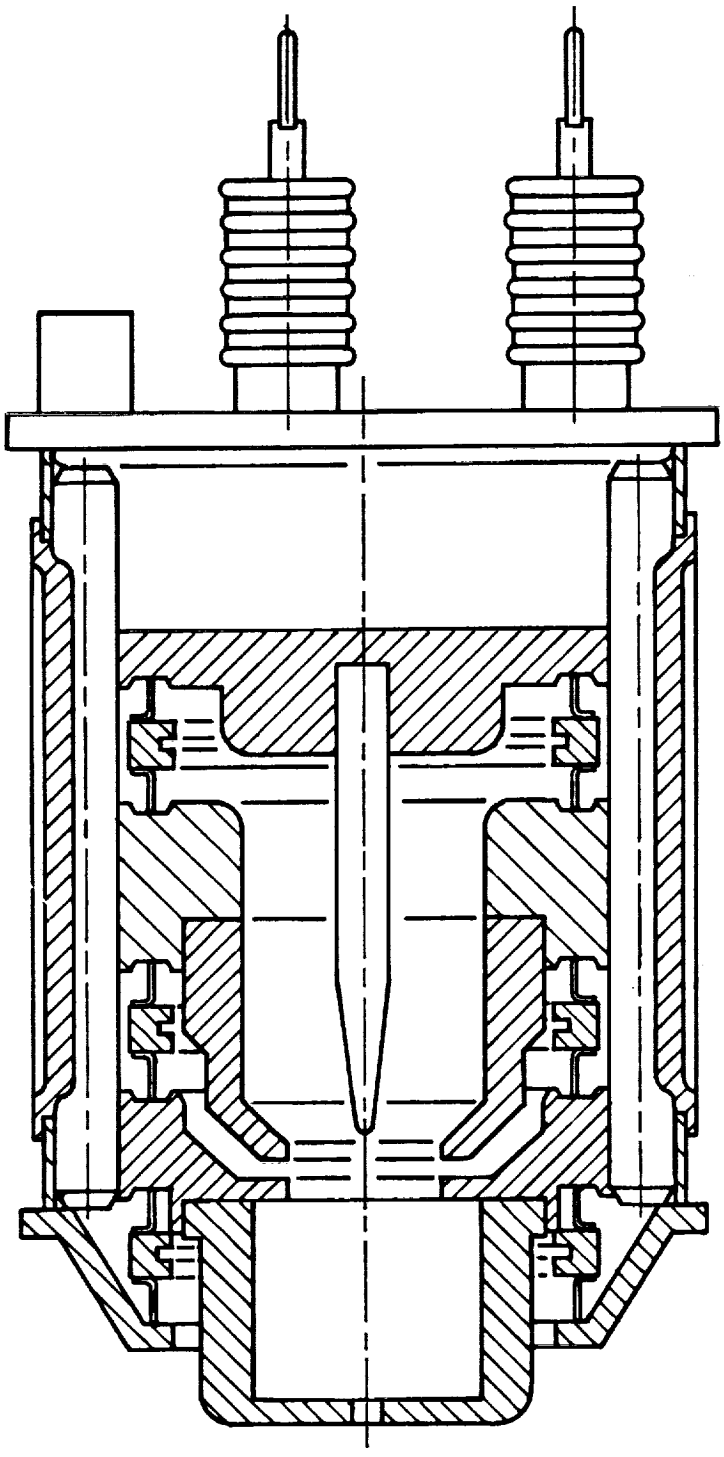

FIGURE 22. COLLECTOR CROSSECTION

The axial field is 3120 to 3700 gauss. The "saddle" in the axial field, predicted in the computer design, does not affect the tube performance and can be reduced by refinements in the magnet design and material. (Time constraints did not permit such refinements for the present program.) The axial field, twice the Brillouin value, is provided over the magnet's 59.8 mm (2.355") gap.

The focusing of the microperveance-0.2 gun in its magnet was verified by building a "beam stick" with a drift region 63.5 mm (2.5") long and minimum tunnel diameter of 0.5 mm (0.020"). On S/N's 101 and 102, the beam transmission at 10 kV was 95%, which was achieved by moving the gun 1.0 mm (0.040") into the magnet, changing the magnetic field entrance conditions. This was the maximum distance the gun could be moved toward the magnet, and the transmission continued to increase, indicating that further movement of the gun toward the magnet pole piece would increase the transmission beyond that achieved in this test. Therefore, the gun nominal position was moved in the proper direction 0.5 mm (0.020") for S/N 103.

4.0 MECHANICAL DESIGN

During the course of this program, the mechanical design of the vacuum assembly was completely modified. This design modification was based on the decision to retain the structural and thermal ruggedness of the previous design, while improving vacuum integrity and making the tube easier to assemble.

Tubes S/N's 101 and 102 proved to be rugged enough to process and test without undue difficulty, and the cooling of S/N 102 was good enough to operate it CW with 209 W rf power out (described in greater detail in Section 6.0). However, one of the vacuum braze joints in S/N 101 leaked so much that it took two attempts to repair it; and after the second attempt, another leak was created when the flange adjacent to the original leak cracked. The second leak could not be repaired and had to be patched with a high-vacuum varnish sealant. Use of this material made it necessary to bake the tube out at 300°C, making it impossible to operate that tube CW. Tube S/N 102 also leaked initially, but the leak was repaired, and the tube was baked-out at 500°C and operated CW. In addition, the final stack-up of the major subassemblies of these tubes was extremely time consuming. Therefore, a design improvement effort was undertaken.

Several steps were taken to improve vacuum integrity. The cooling lines were re-routed so that only a pair of cooling lines were breaking through the vacuum envelope, and those were placed in a portion of the output pole piece assembly where a high reliability braze could be made. In the original design, the most difficult and least reliable braze consisted of a flange through which two rectangular waveguides and two cooling tubes were brazed. In the new design, the cooling lines were removed, the waveguides per flange were reduced from two to one, and the waveguide assembly was modified so that the vacuum braze shape changed from rectangular to circular. In this design, the flanges are heliarced into a body assembly composed primarily of one large, stainless steel cylinder which provides both structural strength and mechanical stability, as well as fewer vacuum brazes. (Most of the vacuum joints are now heliarced, which also reduces the possibility of vacuum leaks.) The rf windows have been designed so that all four are easily accessible for both leak-check and, if necessary, repair. In short, the entire vacuum envelope has been redesigned to be simpler and more reliable.

As indicated above, the improved vacuum reliability was gained without sacrificing structural strength and mechanical stability. The use of the large stainless steel cylinder, coupled with Heliarc joints designed to clamp the subassemblies together, ensures that the entire vacuum assembly is at least as rugged, if not more rugged than before.

The use of a larger outer cylinder also makes easier construction of the final vacuum assembly possible. There is an internal stack composed of the two body assemblies (input and output): an input pole piece assembly and an anode assembly at the gun end; and a similar assembly (called the "tail pipe") along with an output pole piece assembly at the collector end. These assemblies are aligned through the use of coupling rings, each of which is machined with sufficient accuracy to ensure that the alignment of the gun, anode, circuits, and collector continue to provide the excellent beam transmission obtained on the earlier tubes. The stacking of these major subassemblies is enhanced through the use of screws, which are used to ensure that all subassemblies are held tightly together. The screws are drilled through the center to avoid virtual leaks. Screws are also used to tie the waveguide assemblies to their respective circuit body assemblies. Because the outer cylinder is so large, all of these screws can be installed using conventional socket head cap screws and a ball-ended Allen wrench; and since most of the assemblies are also slightly larger than before, they are easier to handle.

The cooling scheme consists of a circular "race" in the output pole piece assembly; a set of tubing connections attached to the inside of that assembly and connected to the race; and a series of tubes connecting the race to the anode, tail pipe, and body assemblies. As implied above, all of these cooling components are completely inside the vacuum assembly. This scheme did not function as intended in the S/N 103 tube, as the pieces of tubing were difficult to connect properly, and the system leaked internally. But this condition did not compromise the ability to put S/N 103 through exhaust, as the leaking portions of the cooling structure were simply sealed off. However, taking this action left some parts of the assembly without water cooling. Actually, the complexity of this cooling scheme may have been unnecessary, as the sheer size of most of the assemblies, coupled with the extensive use of copper, reduces the need for cooling each subassembly separately.

Other construction modifications are discussed in Sections 3.0 to 3.5. The collector and the window, described with emphasis on their potential for improved electrical performance, were also redesigned with improved mechanical performance in mind.

One change also had to be made in the focusing assembly because of the change in the position of the waveguide assemblies: two additional cutouts were necessary in the outer pole piece to make allowances for the waveguides. But this change should not affect focusing, as the outer pole piece is massive enough that the magnetic flux within it is well below saturation, and far enough away from the tube body to avoid any azimuthal disturbance in the axial field.

In summary, the mechanical design modification produced a more reliable tube without compromising any critical design features of earlier designs.

5.0 ASSEMBLY AND TUBE BUILDING

5.1 ASSEMBLY BUILDING

The design described in Section 4.0 was used to build tube S/N 103. Figures 23 through 28 show various subassemblies used on that tube. A number of the assembly processes have been simplified in the new tube design, as shown in Figure 23. The liquid cooling is channeled through the output pole piece assembly, virtually eliminating vacuum wall brazes for the cooling pipes. The external cylinder has been made as large as the existing magnet assembly permits, which makes building up the internal subassemblies much easier; and there is a single waveguide per vacuum flange. The waveguide assemblies shown in Figure 24 are much simpler and less prone to vacuum leaks than their predecessors.

Likewise the anode and tail-pipe assemblies shown in Figure 25 are larger and easier to handle. All of the assemblies shown in Figures 26 and 27 have also been modified with easier handling in mind, so that stacking the circuits and connecting them to the adjacent assemblies has become much easier. The connection between the circuits and the waveguides is simpler too.

A final construction note: the single stage collector used in the first design has been replaced by the multistage depressed collector shown in Figure 28. This collector has two intermediate stages and a probe biased at cathode potential. Though the collector was designed for this particular application, all of its construction techniques conform to standard helix tube assembly practices.

5.2 TUBE BUILDING AND DELIVERY

Two tubes were delivered on this program, S/N's 102 and 103. As indicated in Sections 2.2 and 6.0, S/N 102 was extensively tested. After the testing was completed, the flexible water cooling lines were removed to avoid trapping moisture in the cooling system. The tube, as shipped, is operable if all the cooling and electrical lines are properly connected and insulated. The other tube, S/N 103, was constructed as described in Section 4. It was processed through exhaust, but developed a leak in the output pole piece assembly, which

F580

FIGURE 23. BODY STACK AND CYLINDER FOR S/N 103

F580

FIGURE 24. WAVEGUIDE ASSEMBLY FOR S/N 103

F580

FIGURE 25. ANODE AND TAIL PIPE ASSEMBLY FOR S/N 103

F580

FIGURE 26. SUBASSEMBLIES FOR S/N 103

F580

FIGURE 27. STACKED BODY AND MATING ASSEMBLIES FOR S/N 103

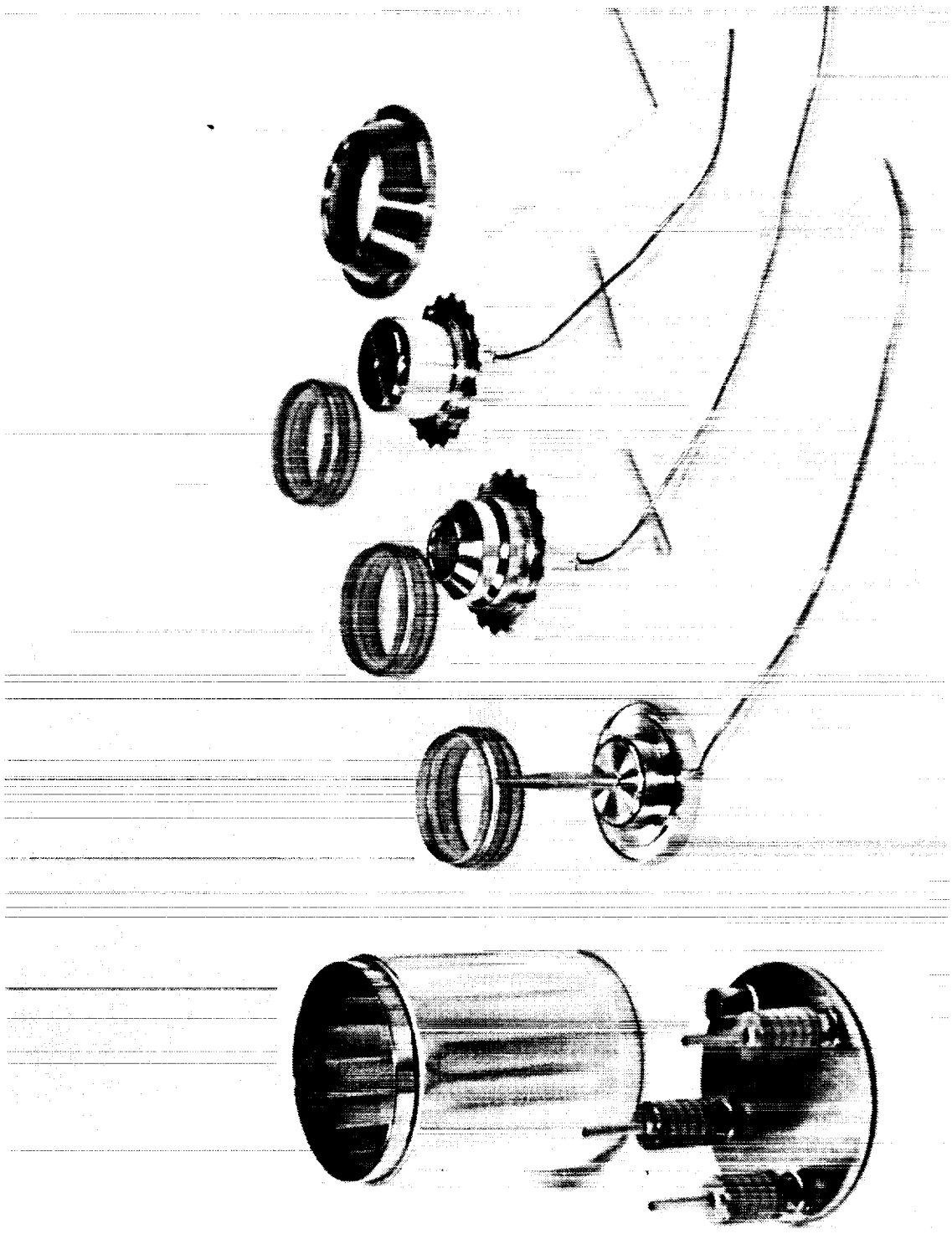

F580

FIGURE 28. MULTISTAGE-DEPRESSED COLLECTOR SUBASSEMBLIES FOR S/N 103

was patched with a low vapor pressure, high-temperature epoxy. After exhaust was completed, another problem related to performance was found. The rf output match was much worse than before exhaust. This same problem was also observed prior to testing S/N 102. However, when that tube was operated at 1 percent duty for a few hours, the match improved until the VSWR was about 2:1, leading to the conclusion that the poor match was caused by metal deposited on the diamond insulators during exhaust. The metal then evaporated during preliminary rf testing, and was redeposited elsewhere in the tube.

To test S/N 103 , it would have to be placed in the appropriate magnet assembly, have its high-voltage electrodes properly connected and insulated, and have its cooling system connected to a source of coolant. The last two requirements are straightforward. The first requirement requires special equipment, as the magnetic forces involved are great, and the tube would most likely be damaged if the magnets became misaligned during assembly. Despite these restrictions, S/N 103 is capable of being tested, should the opportunity arise to follow the steps briefly outlined above.

6.0 TUBE DATA

Tube S/N 102 was tested for average power performance. Because this tube had low gain, it could not be driven into the large-signal region with the +30 dBm available. Therefore, double-stub tuners were mounted at both the input and output sever ports. When the tuners were adjusted for maximum power, over 200 W CW output power was obtained. However, the use of the tuners made the tube very phase sensitive, and it was not possible to take power in/power out transfer curves. As soon as the rf drive was varied more than 3 dB, the output power shifted suddenly and substantially. In addition, these changes were not reversible, probably due to phase-locking. Despite all of these problems, the following performance was obtained:

Cathode Voltage	-9.75 kV
Cathode Current	205 mA
Collector Voltage (wrt cathode)	8.6 kV
Body Current (without drive)	20 mA
(with drive)	30 mA
RF Input Power	+27 dBm
RF Input Frequency	28.33 GHz
RF Output Power	53.2 dBm (209 W)

This set of data indicates clearly the ability of the tube to operate under high average power conditions. For example, the body current power dissipation is 195 W without drive, and nearly 292 W with drive. (Under these conditions the body power is not the product of cathode voltage and body current, as some electrons have been slowed down.) In addition, if the circuit efficiency is 80 percent the rf power dissipated at 209 W power is 52 W. The body current power dissipation may occur only on the anode and tail pipe, both of which are massive copper structures, and not on the circuit; but the rf power must be dissipated on the circuit, indicating that the bonds are very reliable between the circuit rungs, which are 0.064 mm (0.0025") x 0.165 mm (0.0065") in cross section, and the diamond supports; and between the rungs and the cavity walls.

7.0 CONCLUSIONS

The results of the work undertaken on this program included the following accomplishments:

- Refinements to the electrical design which provide higher gain, better centering on the desired frequency band, higher tube efficiency, and a greater assurance of mode-free operation.

- Refinements to the mechanical design which ensure greater vacuum integrity and easier stacking of subassemblies, while at the same time maintaining rugged thermal and mechanical constructions.

- The building and exhaust of S/N 103 which verifies the usefulness of the mechanical refinements.

- The high average power testing of S/N 102, which verifies the intrinsic power-handling capability of the structure. The tests done on S/N's 101 and 102 demonstrate the intrinsically repeatable performance that was expected from the chemically milled ladder structures.

While the electrical and mechanical viability of the TunneLadder has been demonstrated, the ability to produce such tubes inexpensively remains elusive. Many circuit subassemblies were produced successfully on the first try. However, when brazes were not complete, the problems generally occurred at the circuit ends. Every circuit assembly was successfully completed on re-braze, but the extra braze steps consumed time and resources. As with any device that uses several new techniques, the initial construction efforts were costly. However, the experience gained in fabricating assemblies indicates that the learning curve should be relatively steep, and the likelihood of building competitively priced devices that operate in the linear region at 200 W CW with up to 3 percent bandwidth in Ka-band appears possible.

8.0 RECOMMENDATION

At this time, whether or not to proceed with the development of tubes using a TunneLadder circuit depends on two criteria: 1) the need for devices meeting the performance characteristics cited earlier, and 2) the availability of other devices which can provide the same performance. Assuming that the first criterion is met, one must examine the second. Here, an argument supporting further development is less clear. Both conventional helix and derivations of coupled-cavity tubes have been built which may, at the present time, have better performance. The question that remains is whether or not the TunneLadder has the potential for performance superior to these alternates and, if so, whether or not it is practical to pursue such performance.

Assuming that such a course of action is practical, the following efforts are recommended:

1. Additional redesign of mechanical structure. This effort might include putting the structural supports outside the vacuum assembly.

2. Replacement of the waveguide couplers at the ends of the body sections with internal terminations.

3. Redesign of the magnetic focusing structure. The gap between the gun and the collector pole pieces could be shortened, resulting in a smaller magnet. This goal could also be reached with the higher energy materials now available.

4. Design of a PPM focusing structure. This effort would take advantage of the work suggested in Item 1 above.

5. Incorporation of the design techniques developed for other millimeter-wave TWTs.

6. Simplification of the diamond supports.

7. Further investigation of electron beam etching.

Pursuing all of the paths would eventually lead to a practical, high-average power, millimeter-wave device.

9.0 REFERENCES

1. A. Karp, "Traveling Wave Tube Experiments at Millimeter Wavelengths with a New, Easily Built, Space-Harmonic Circuit, " Proc. I.R.E., vol. 43, pp. 41-46, (1955).

2. A. Karp, "Design Concepts for a High-Impedance Narrow Band 42 GHz Power TWT Using a 'Fundamental/Forward' Ladder-Based Circuit," Final Report, Varian Associates, Inc., Palo Alto, CA, February 1981 (NASCR-165282).

3. H. Kosmahl, R. Palmer, "Harmonic-Analysis Approach to the 'TunneLadder' A Modified Karp Circuit for Millimeter-Wave TWTAs," IEEE Trans. Electron Devices, Vol. ED-29, pp. 862-869, May 1982.

4. A. Karp, "Millimeter- Wave Valves," pp. 73-128 in Fortschritte der Hochfrequenztechnik, Vol. 5, M. Strutt et al., eds., Academic Press MBH, Frankfurt/Main, 1960.

5. Ibid., Figure 30 (d), p. 116.

6. Ibid., Figure 30 (e), p. 116.

7. Ibid., bibliography items 118-123, p. 127.

8. A. Karp, "Backward-Wave Oscillator Experiments at 100 to 200 kilomegacycles," Proc. I.R.E., Vol. 45, pp. 496-503 (1957).

9. L.D. Cohen, "Backward-Wave Oscillators for the 50 to 300 GHz Frequency Range," IEEE Trans. Electron Devices, Vol. ED-15, pp. 403-404, June 1968.

10. See Reference 4, Figure 30 (c), (f), and (h), p. 116.

11. Ibid, bibliography items 130a, 131, p. 127.

12. J.R. Pierce, Traveling-Wave Tubes, D. Van Nostrand Co., New York, 1950; Figure 5.7, p. 90.

13. J.R. Pierce, "Propagation in Linear Arrays of Parallel Wires,: I.R.E. Trans. Electron Devices, Vol. ED-2, pp. 13-24 (1955).

14. See Reference 4, bibliography items 125, 127, and 128, p. 127.

15. H.G. Kosmahl and T. O'Malley, "Harmonic Analysis of the Forward-Wave Karp Circuit as a Millimeter-Wave Amplifier in the 100-500 W Range," Microwave Power Tube Conference, Monterey, CA, 3 May 1978.

16. Ibid.

17. A. Karp, "Design Concepts for High-Impedance Narrow Band 42 GHz Power TWT Using a 'Fundamental/Forward' Ladder-Based Circuit," Final Report, Varian Associates, Inc., Palo Alto, CA, February 1981 (NASCR-165282).

18. A Jacques, A. Karp, D. Wilson, and A. Scott "A Millimeter-Wave TunneLadder TWT," Final Report, Varian Associates, Inc., Palo Alto, July 1985, (NAS-3-22466).

NASA
National Aeronautics and Space Administration

Report Documentation Page

1. Report No.	2. Government Accession No.	3. Recipient's Catalog No.
CR 182183		

4. Title and Subtitle
A Millimeter-Wave Tunneladder TWT

5. Report Date
June 1987

6. Performing Organization Code

7. Author(s)
D. Wilson

8. Performing Organization Report No.

10. Work Unit No.
506-61-42

9. Performing Organization Name and Address
Varian Associates
Microwave Tube Division
611 Hansen Way
Palo Alto, CA 94303

11. Contract or Grant No.
NAS 3-23347

13. Type of Report and Period Covered
Final Report
Oct 1982 - Jan 1986

12. Sponsoring Agency Name and Address
Lewis Research Center
21000 Brookpark Road
Cleveland, OH 44135

14. Sponsoring Agency Code

15. Supplementary Notes
Lewis Research Center Contract Manager,
Peter Ramins, Space Electronics Division

16. Abstract

A millimeter-wave TWT was developed using a dispersive, high-impedance forward wave interaction structure based on a ladder, with non-space-harmonic interaction, for a tube with high gain per inch and high efficiency. The "TunneLadder" interaction structure combines ladder properties modified to accommodate Pierce gun beam optics in a radially magnetized PM focusing structure. The development involved the fabrication of chemically milled, shaped ladders diffusion brazed to diamond cubes which are in turn active-diffusion brazed to each ridge of a doubly ridged waveguide. Cold-test data, representing the $\omega\beta$ and and impedance characteristics of the modified ladder circuit, were used in small and large-signal computer programs to predict TWT gain and efficiency. The structural design emphasizes ruggedness and reliability. Actual data from tested tubes verify the predicted performance while providing broader bandwidth than expected.

17. Key Words (Suggested by Author(s))	18. Distribution Statement
Traveling Wave Tube Tunne Ladder Structure Diamond Supports	Publicly Available

19. Security Classif. (of this report)	20. Security Classif. (of this page)	21. No of pages	22. Price*

NASA FORM 1626 OCT 86

*For sale by the National Technical Information Service, Springfield, Virginia 22161